HQA Lecture 18

I. Friedel oscillations

II. Spin lattices

III. Walkers on gentle slopes

Hydrodynamic spin lattices

Article

Emergent order in hydrodynamic spin lattices

https://doi.org/10.1038/s41586-021-03682-1

Received: 6 July 2020

Accepted: 1 June 2021

Pedro J. Sáenz[1,2]✉, Giuseppe Pucci[2,3], Sam E. Turton[2], Alexis Goujon[2,4], Rodolfo R. Rosales[2], Jörn Dunkel[2] & John W. M. Bush[2]✉


7 June, 2021
nature
Liquid spin lattices
Remarkably tunable
Copenhagen
Something rotten
Many Worlds
RIP
Particle physics
Still not interested
naturejobs Chicago for energy

Effect of outer layer thickness

- adopt the geometry considered in the Friedel oscillations analog

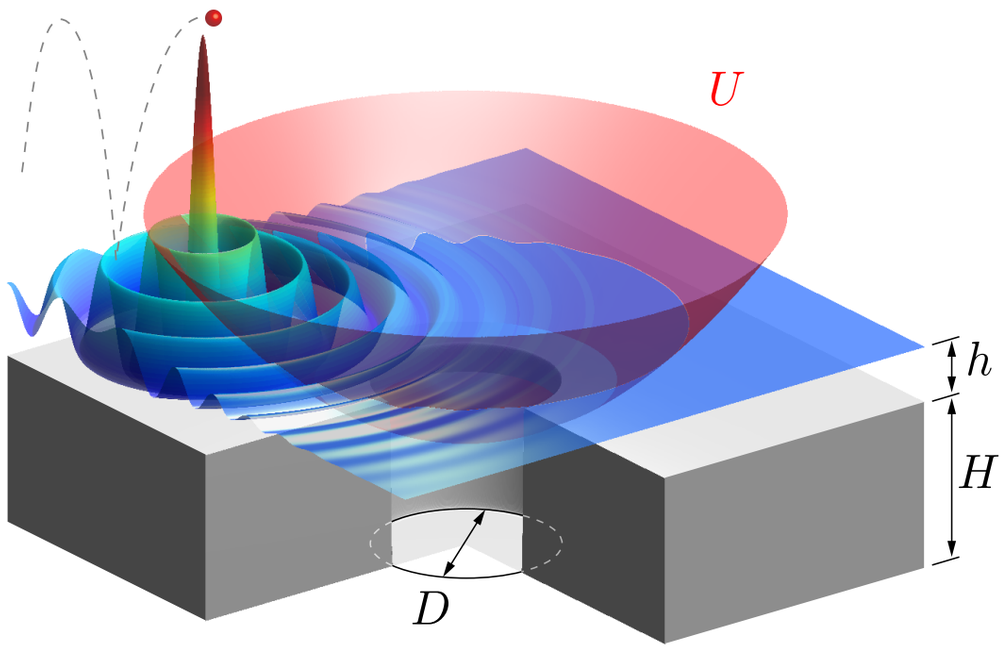

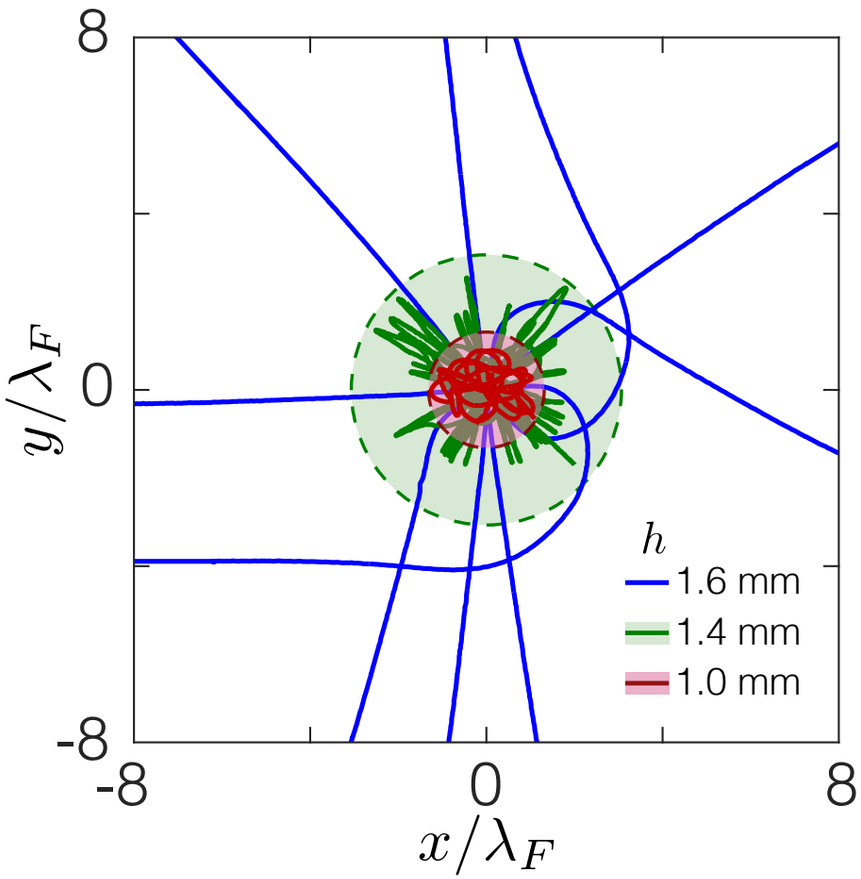

Tighter trapped states emerge for decreasing liquid heights!

Variable bottom topography

Bottom topography can be exploited to induce effective attractive potentials.

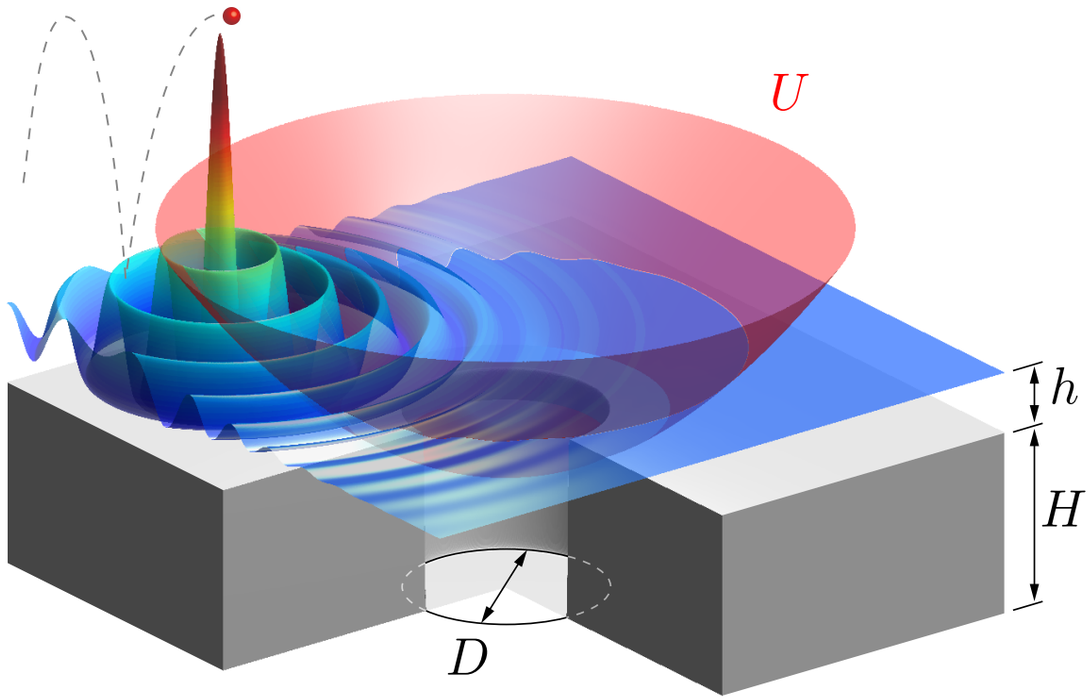

$D \sim 10\,\mathrm{mm}$ $\quad$ $h \sim 1\,\mathrm{mm}$

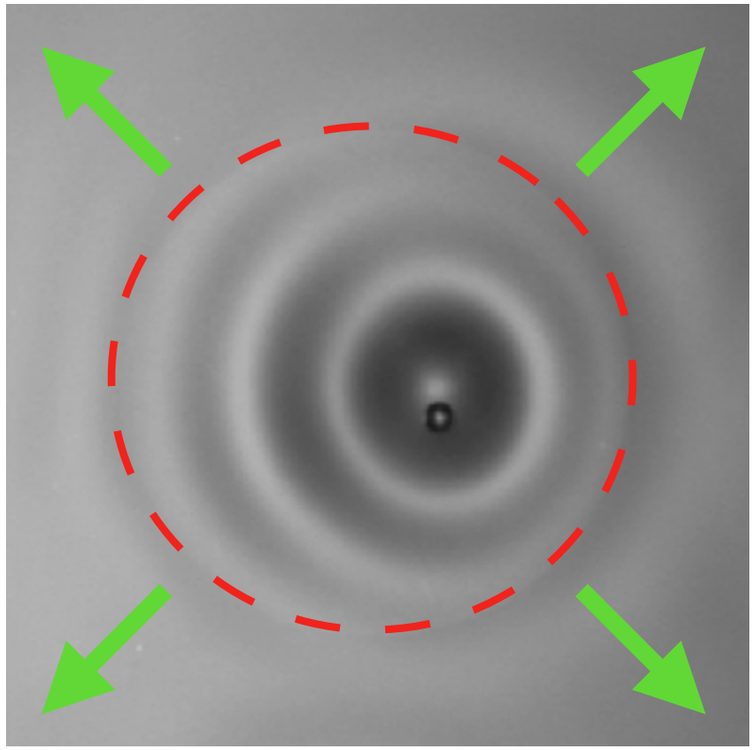

Drop trapped over a submerged well

A submerged well may serve to stabilize a hydrodynamic **“spin state”**

Effect of memory on individual spin states

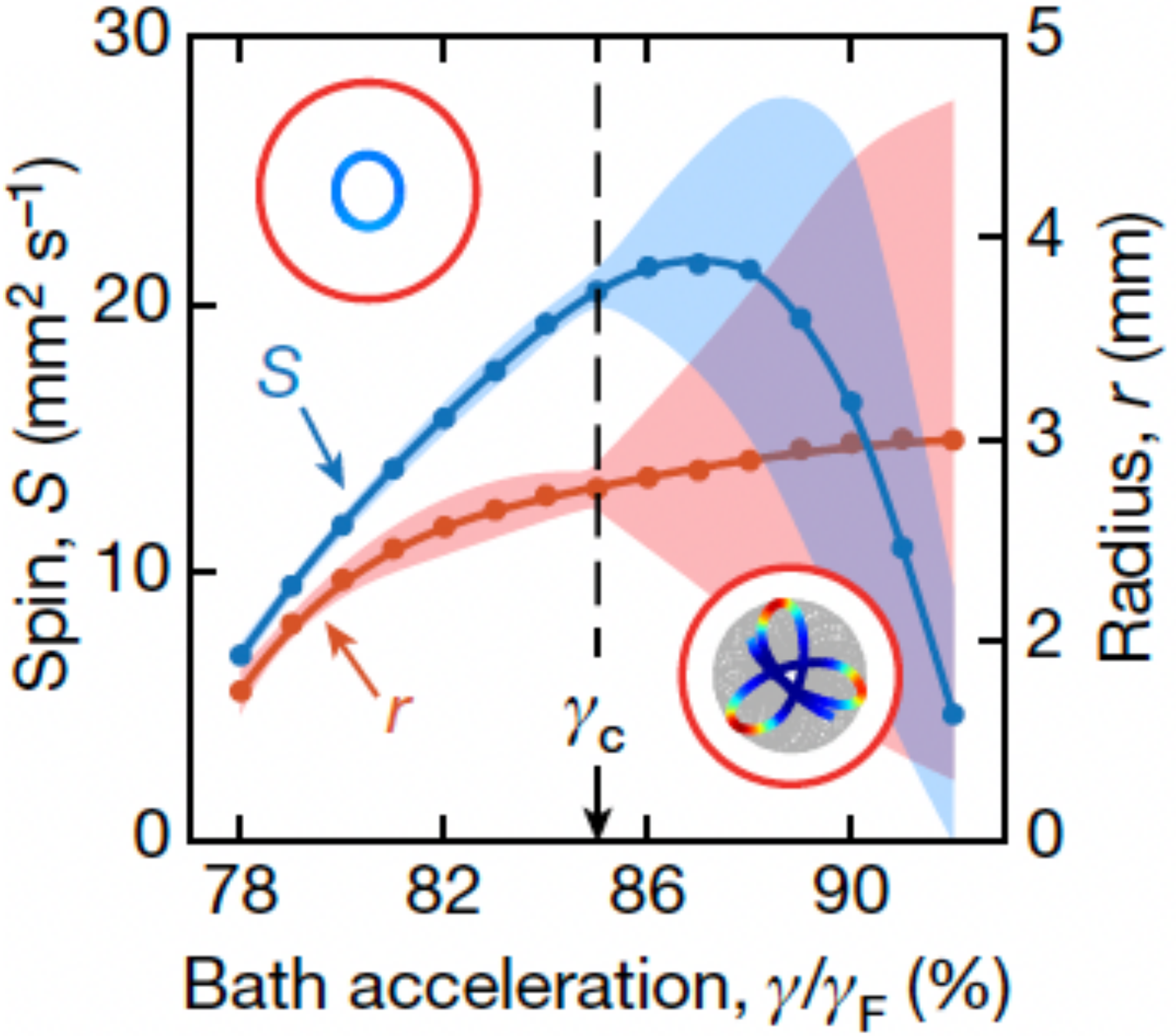

- circular spin states destabilize to wobbling trefoils at high memory

SPIN LATTICES OF WALKING DROPLETS

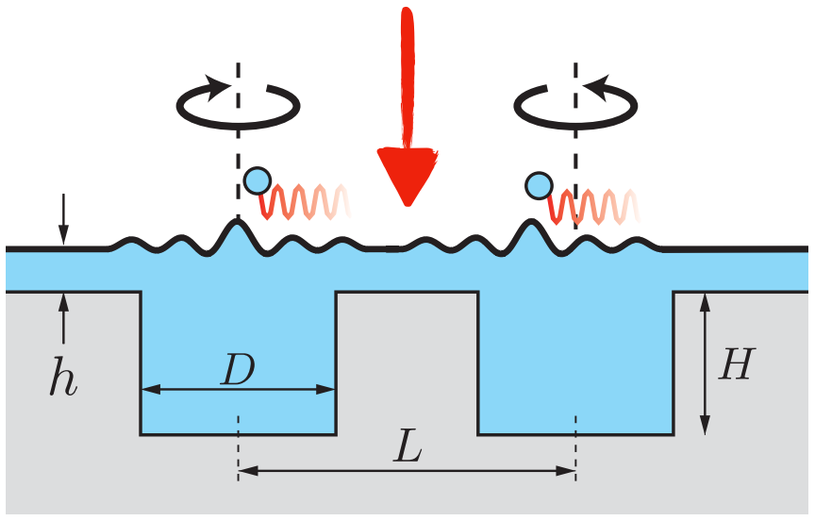

Control parameters

- Geometry h, L, D
- Vibrational acceleration γ/γ_F
- Drop size
- Frequency

Spin dynamics become coupled through
wave-mediated interactions!

The pair-pair coupling can be controlled through several parameters

CHARACTERIZING COLLECTIVE BEHAVIOR

1D lattices

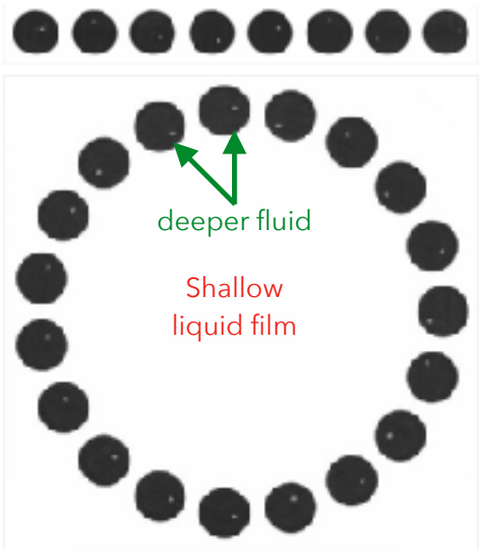

Periodic BCs

2D lattices

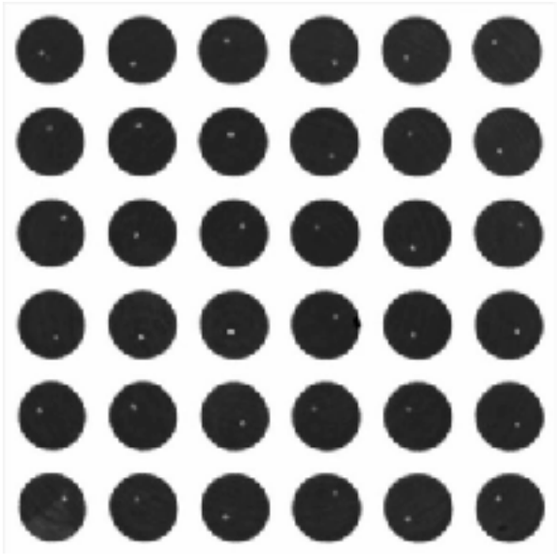

Drop Spin

$$S_i = \frac{\vec{L}_i}{|\vec{L}_i|}$$

CW

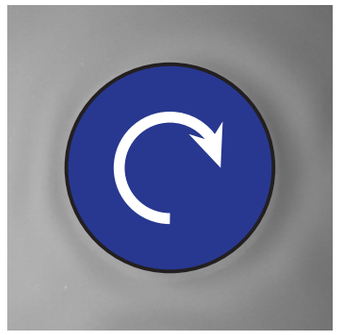

$S = -1$

ACW

$S = +1$

Spin-spin correlation

$$\chi = \langle S_i, S_j \rangle = \frac{1}{N} \sum_{i \sim j} S_i S_j$$

$i \sim j$: nearest neighbors

N : number of pairs

Magnetization $M = \sum_{i=1}^{N} S_i$

Limiting configurations

Ferromagnetic order

$\chi = +1$

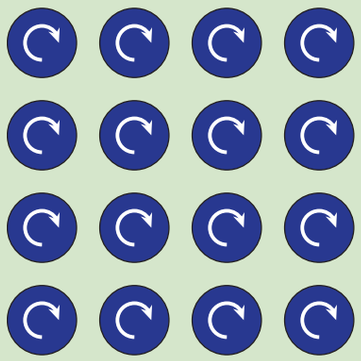

Antiferromagnetic order

$\chi = -1$

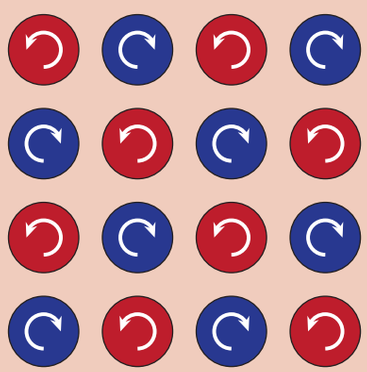

The influence of bouncing phase on spin correlations

- correlations most pronounced when all droplets are bouncing in phase

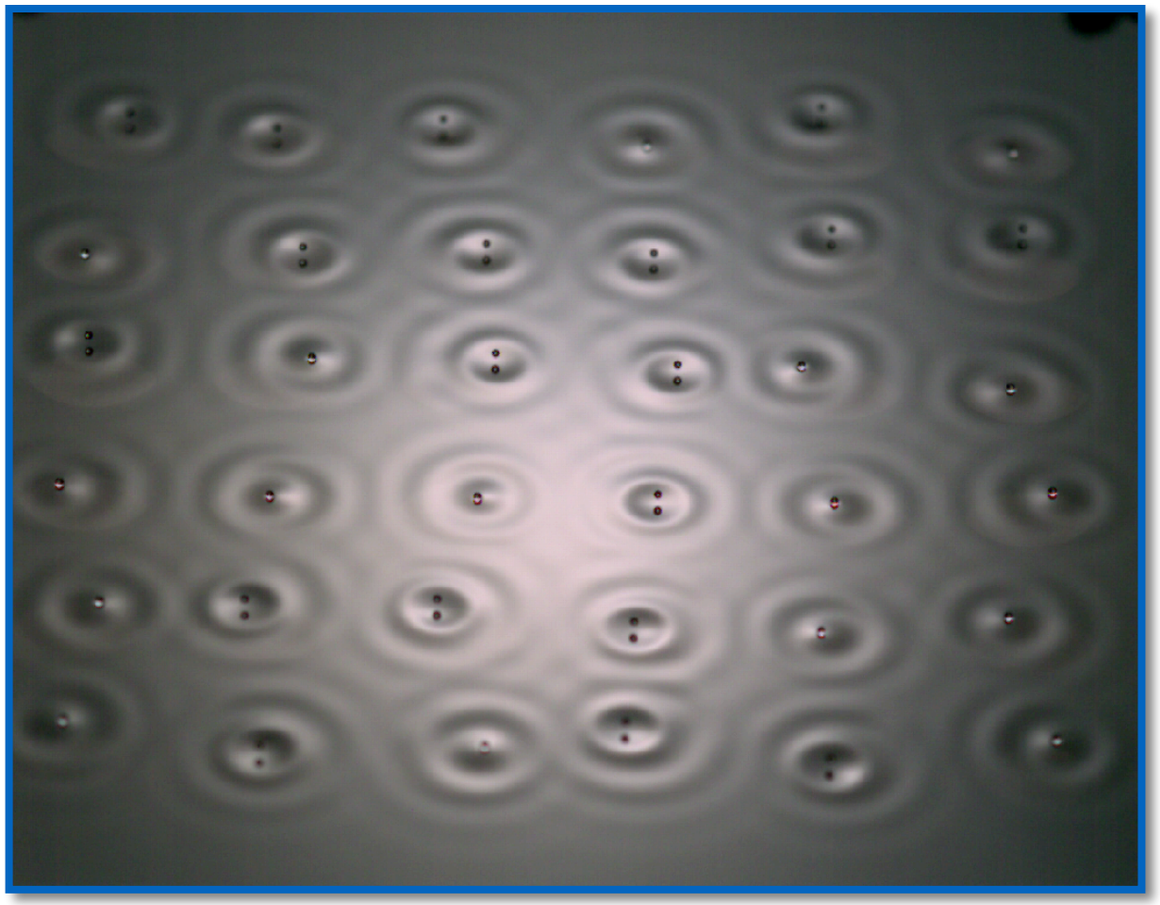

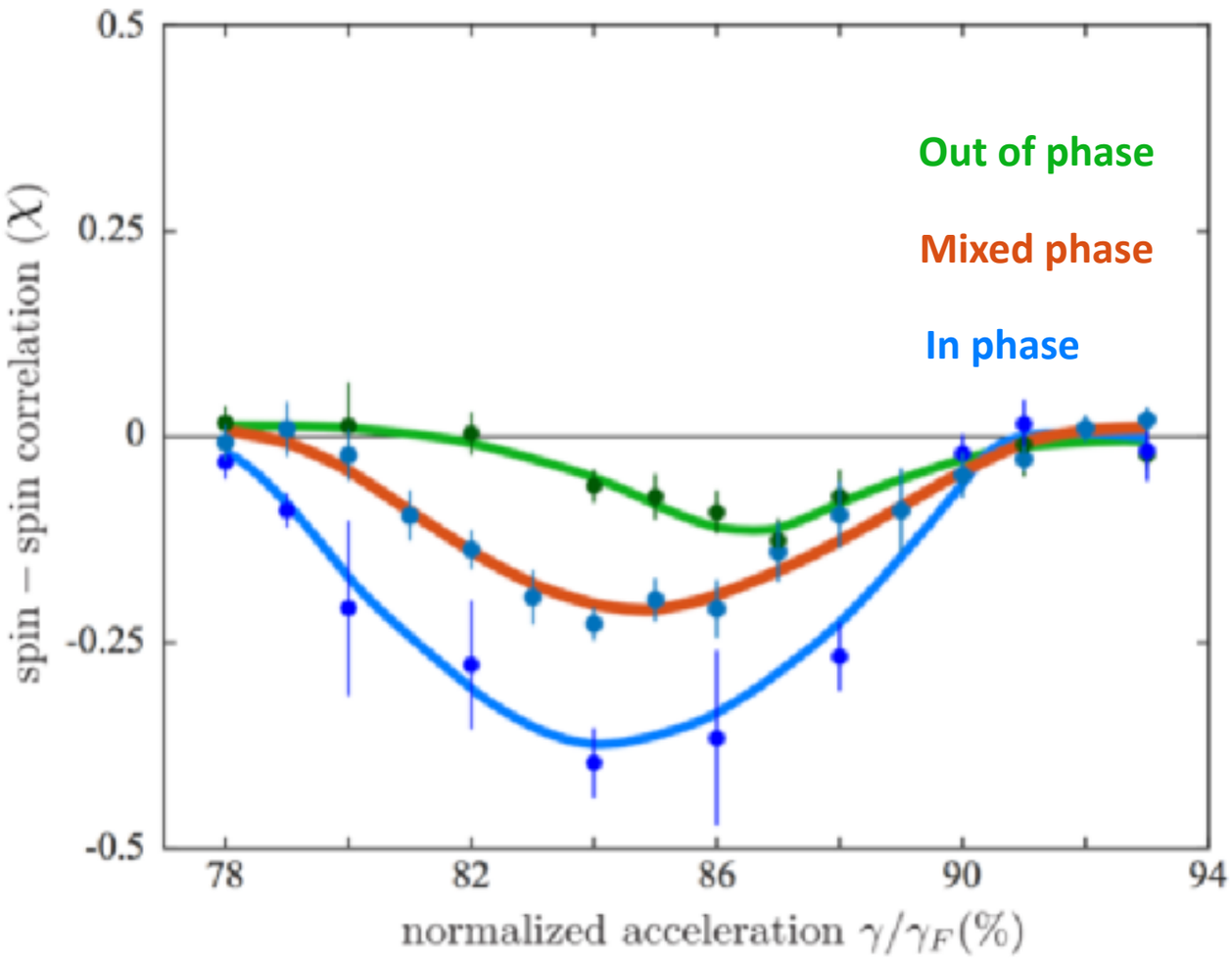

Varying vibrational acceleration

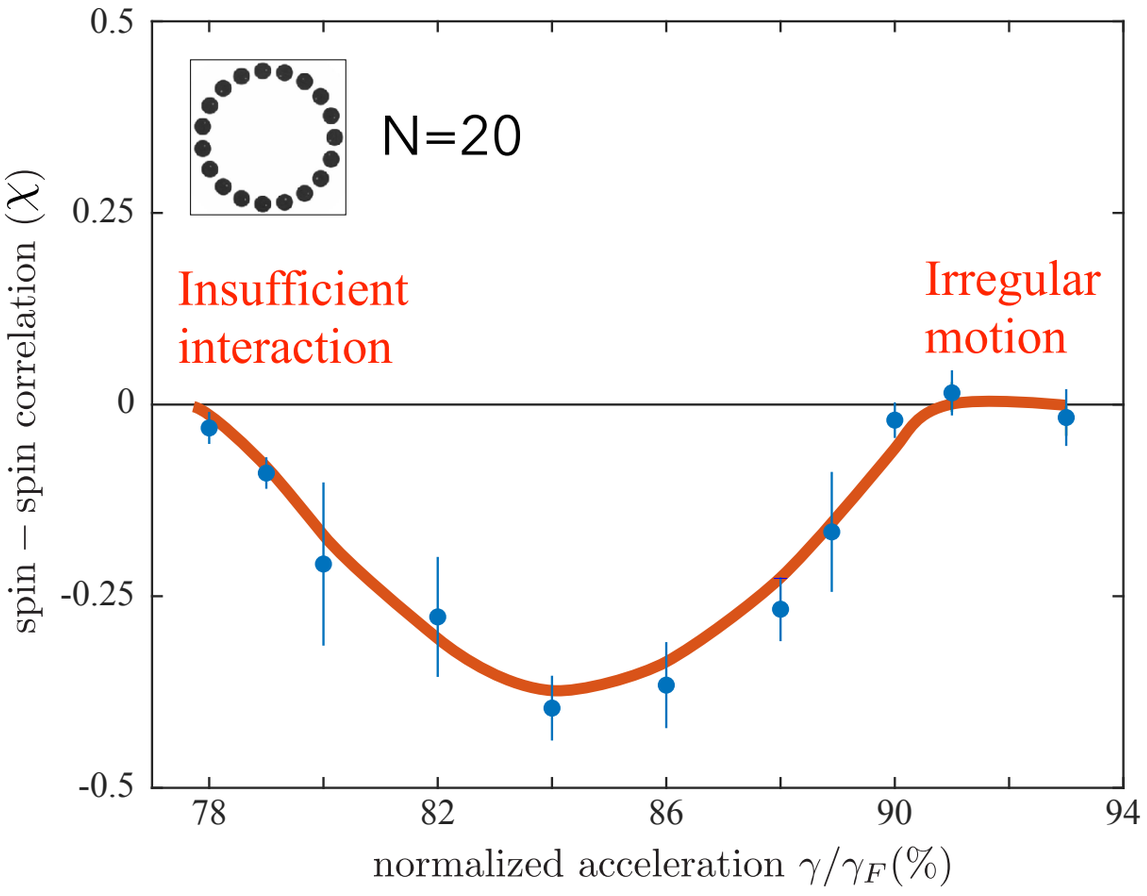

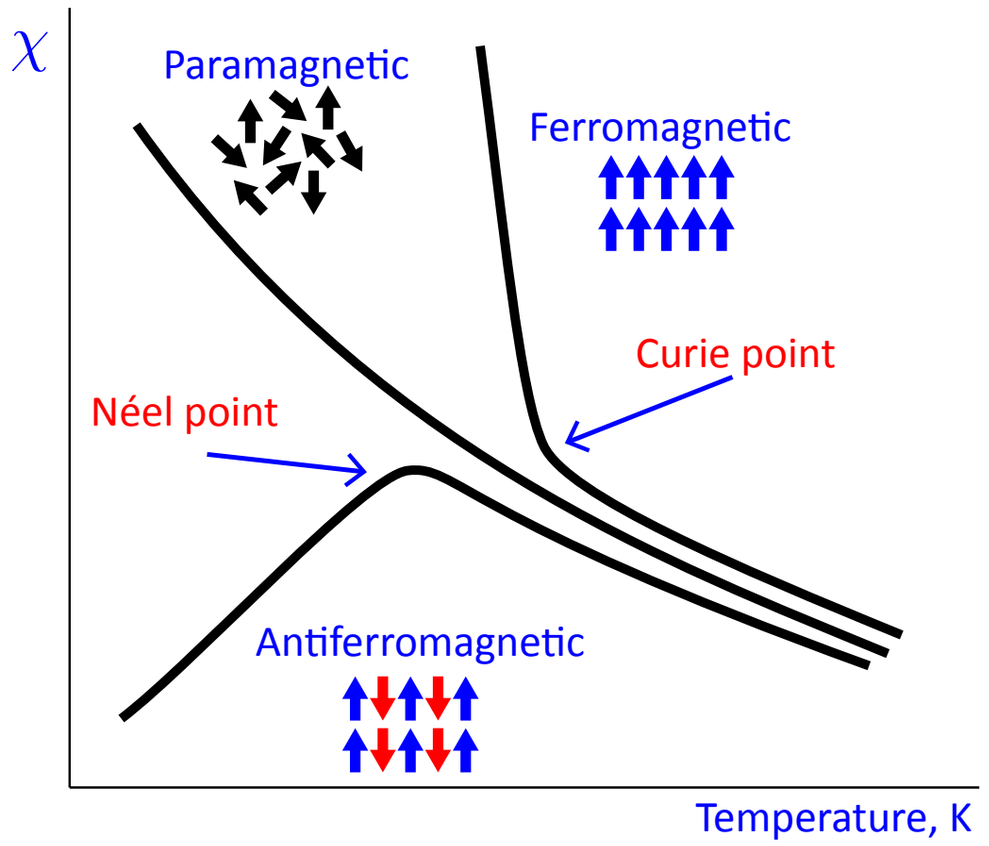

Antiferromagnetic order

$\chi = -1$

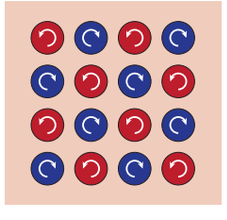

Ferromagnetic order

$\chi = +1$

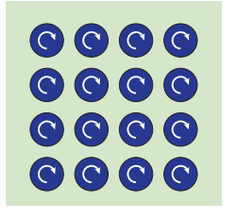

Vibrational acceleration plays the role of an effective temperature.

$$L = 17.7 \text{ mm}$$

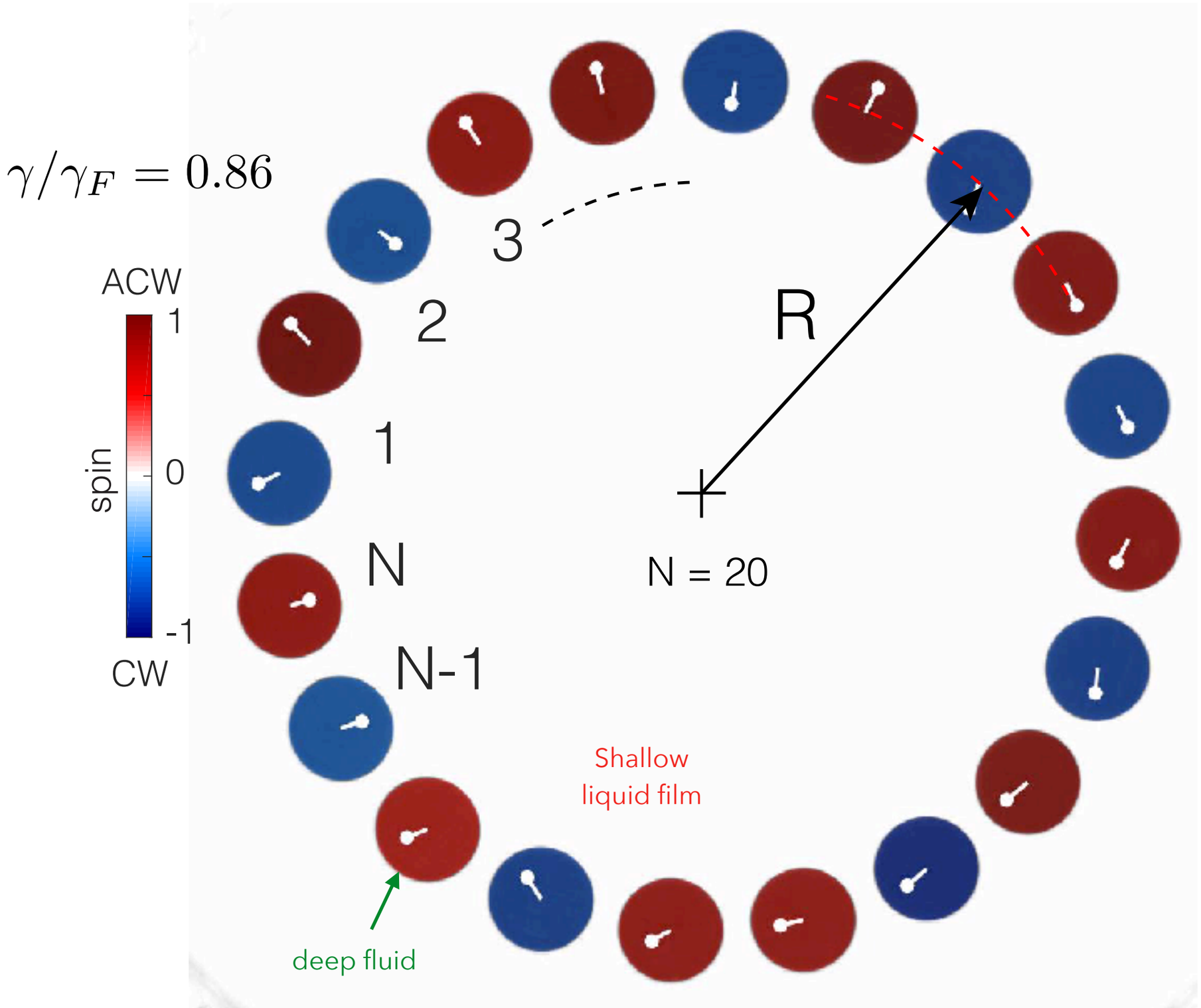
$\gamma/\gamma_F = 0.86$
ACW
1
0
-1
CW
spin
1
2
3
N
N-1
R
N = 20
Shallow
liquid film
deep fluid

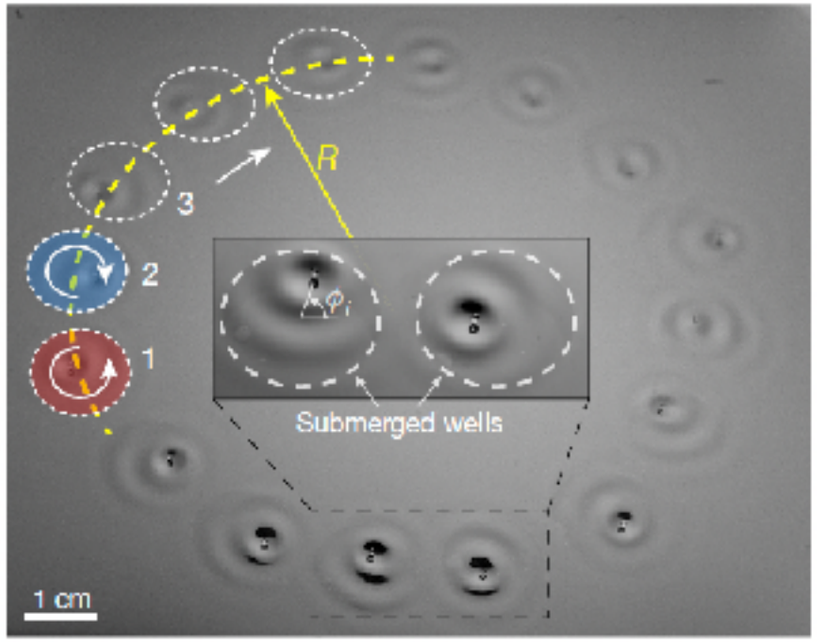

$L = 17.7$ mm

$\gamma/\gamma_F = 0.82$

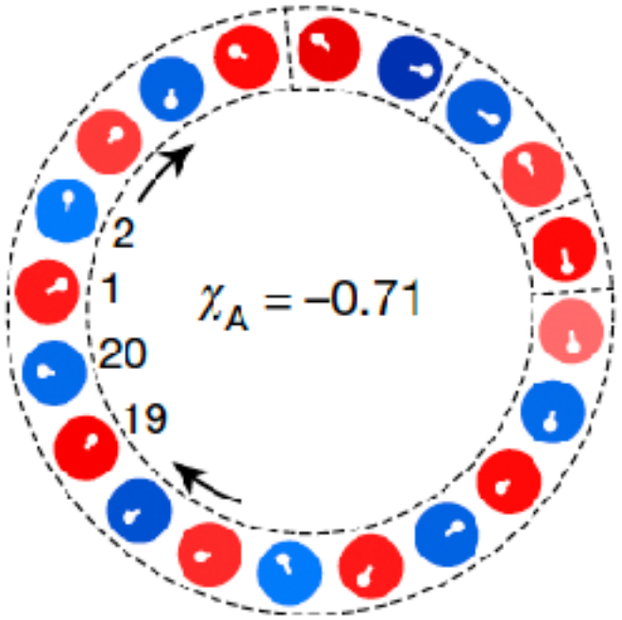

Preferred antiferromagnetic order

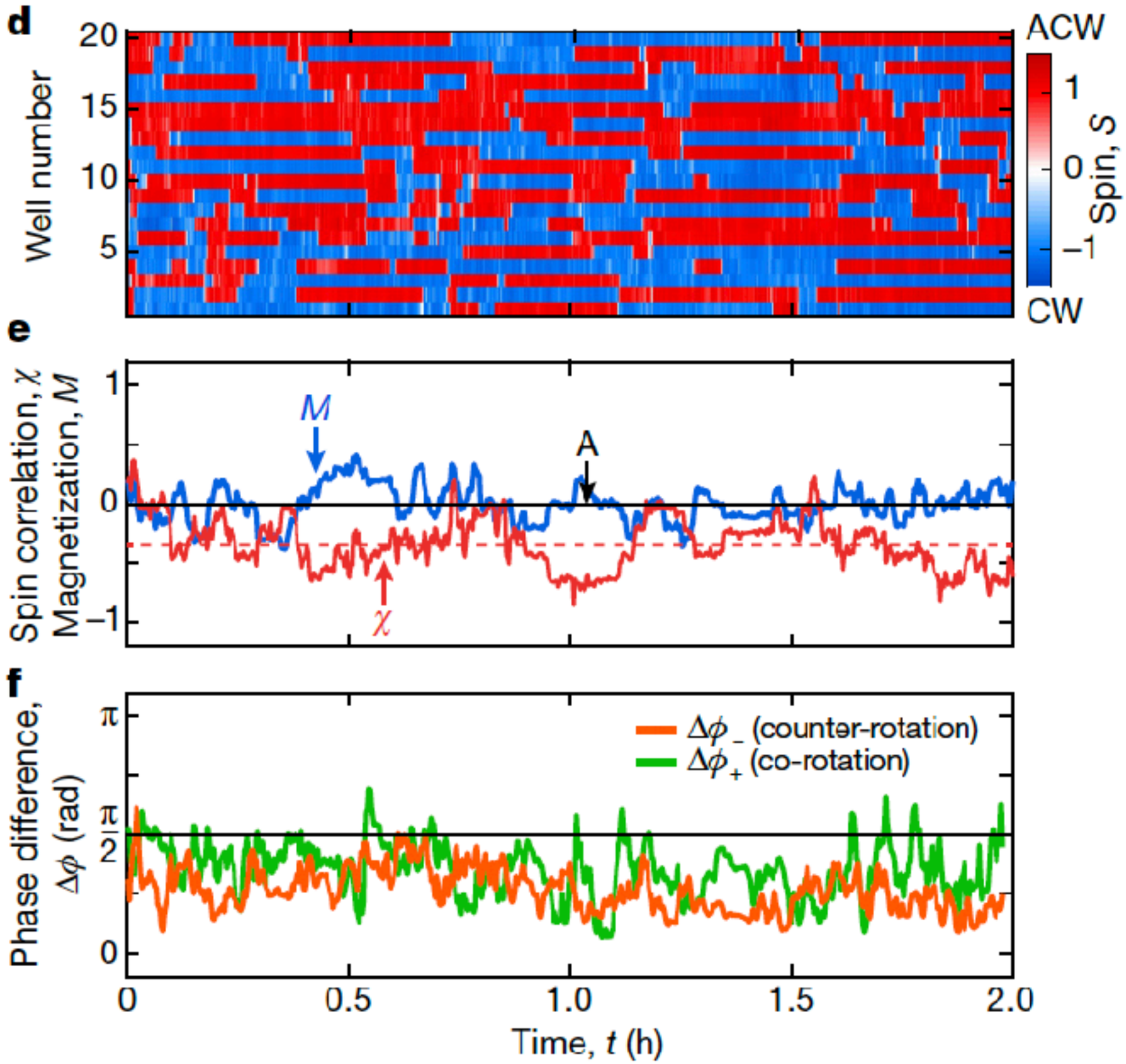

$$L = 17.7 \text{ mm} \qquad \gamma/\gamma_F = 0.86$$

- fix geometry, increase memory slightly

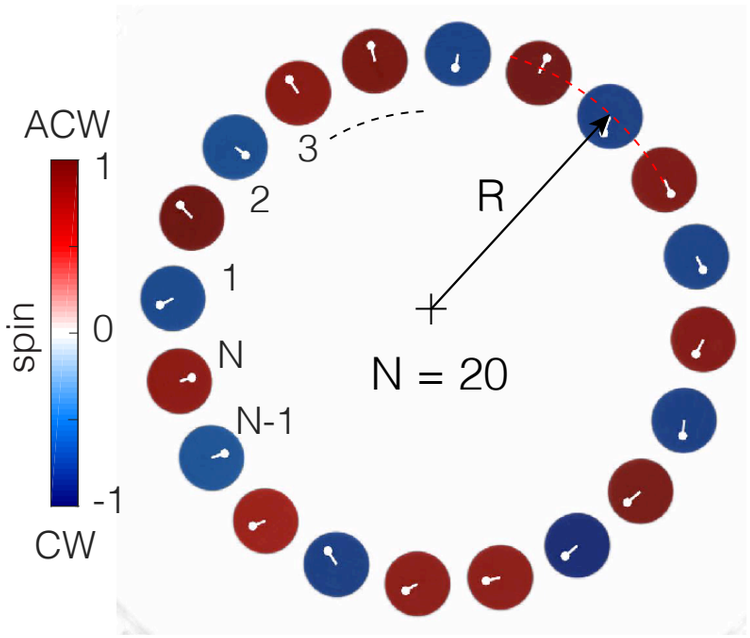

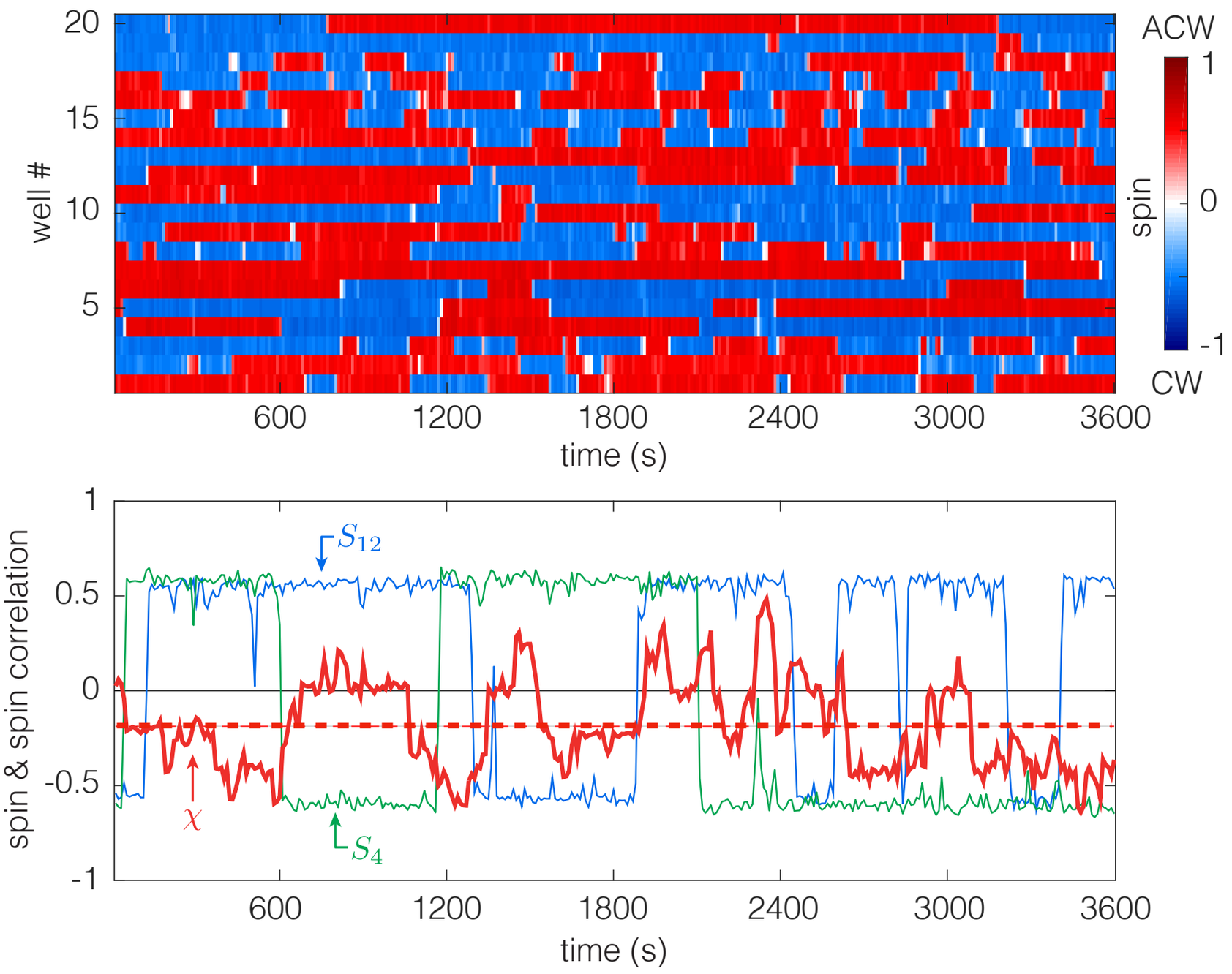

Preferred antiferromagnetic order

$L = 13.2\ \mathbf{mm}$ $\quad \gamma/\gamma_F = 0.86$

- fix memory, alter lattice spacing L

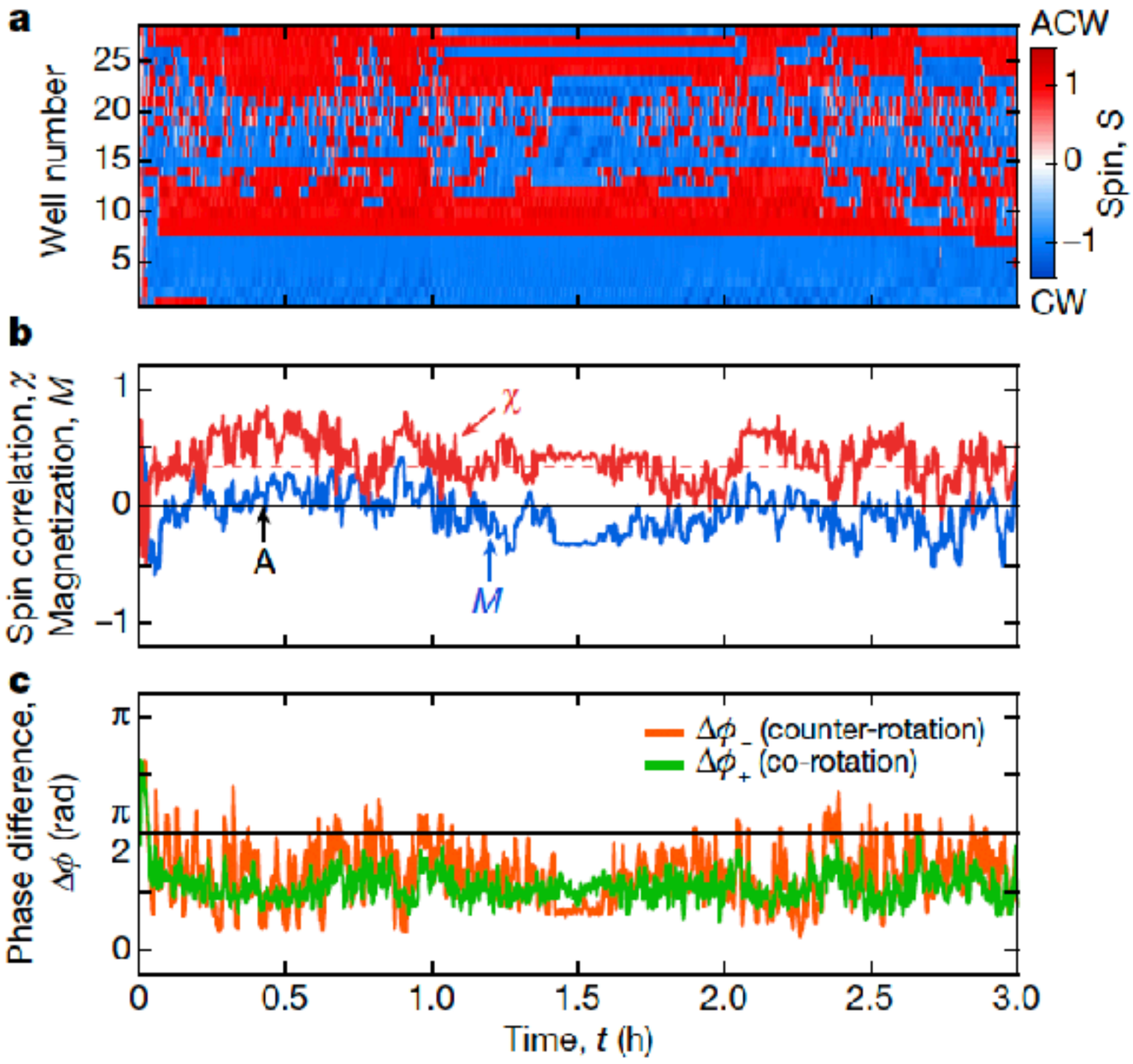

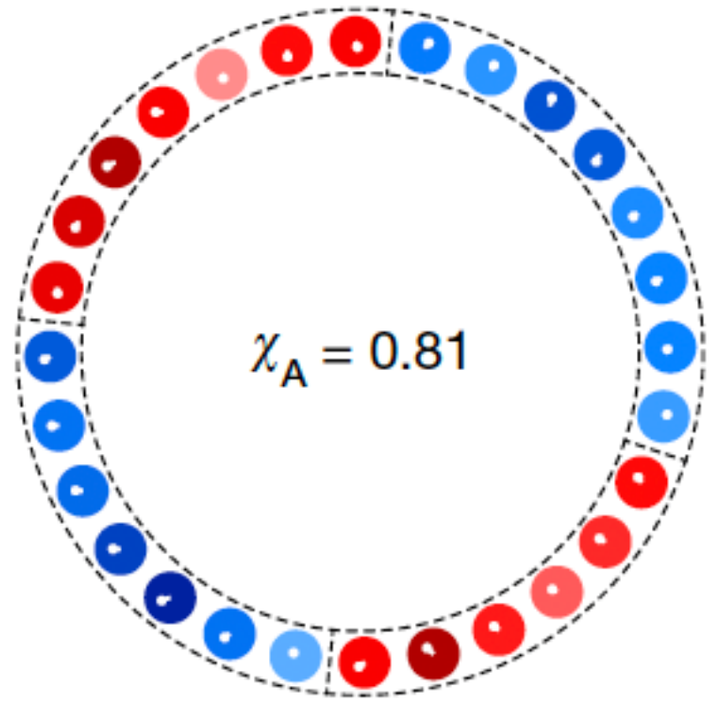

Preferred ferromagnetic order

$\gamma/\gamma_F = 0.86$

VARYING WELL SPACING

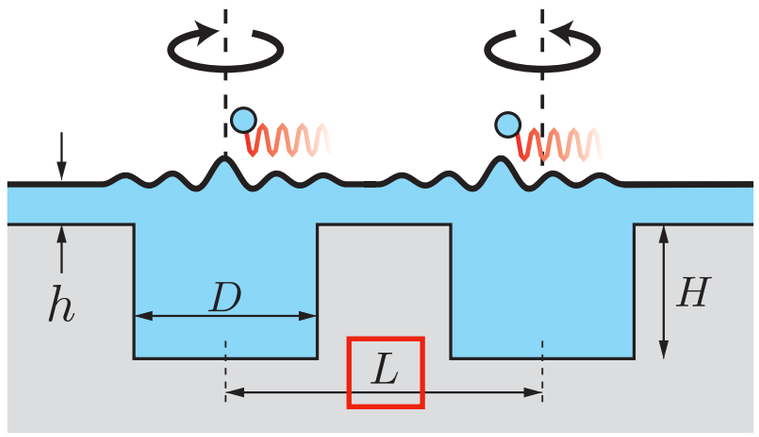

Transition through lattice spacing!

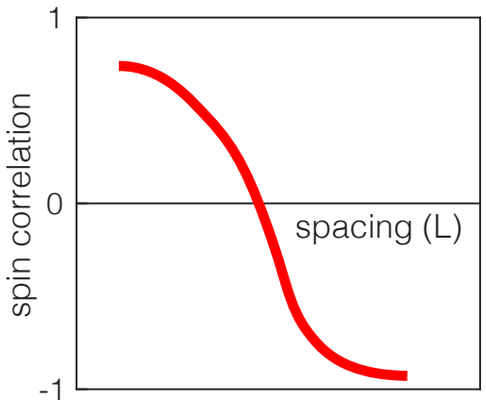

$L = 17.7$ mm

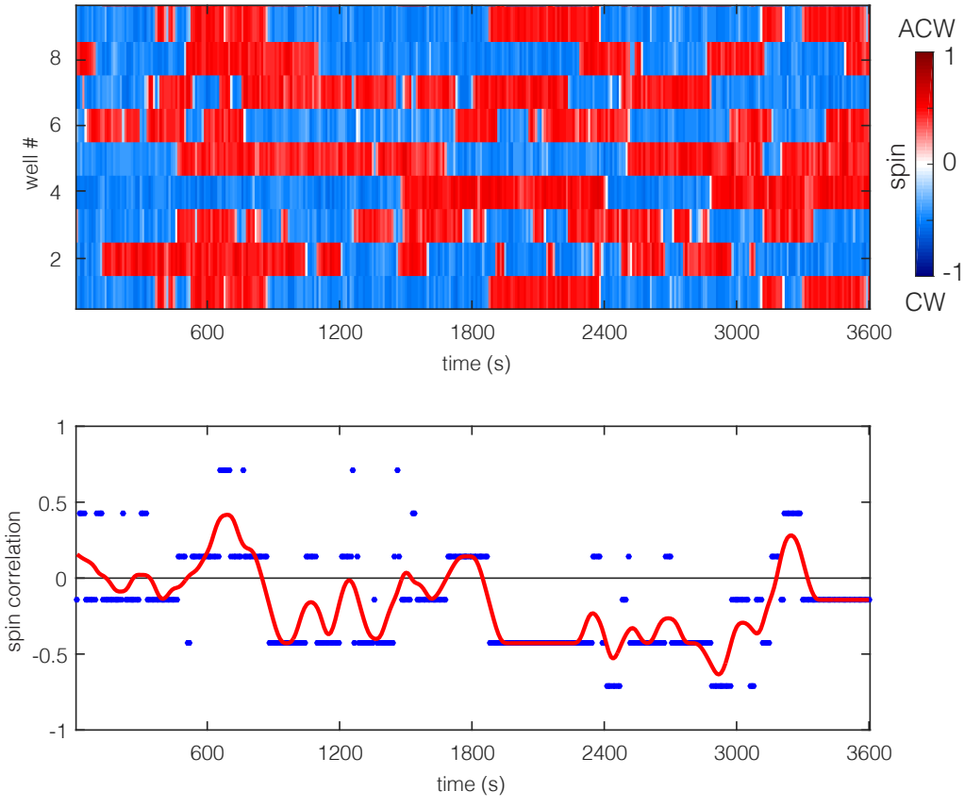

antiferromagnetic

$\langle \chi \rangle < 0$

$L = 14.9$ mm

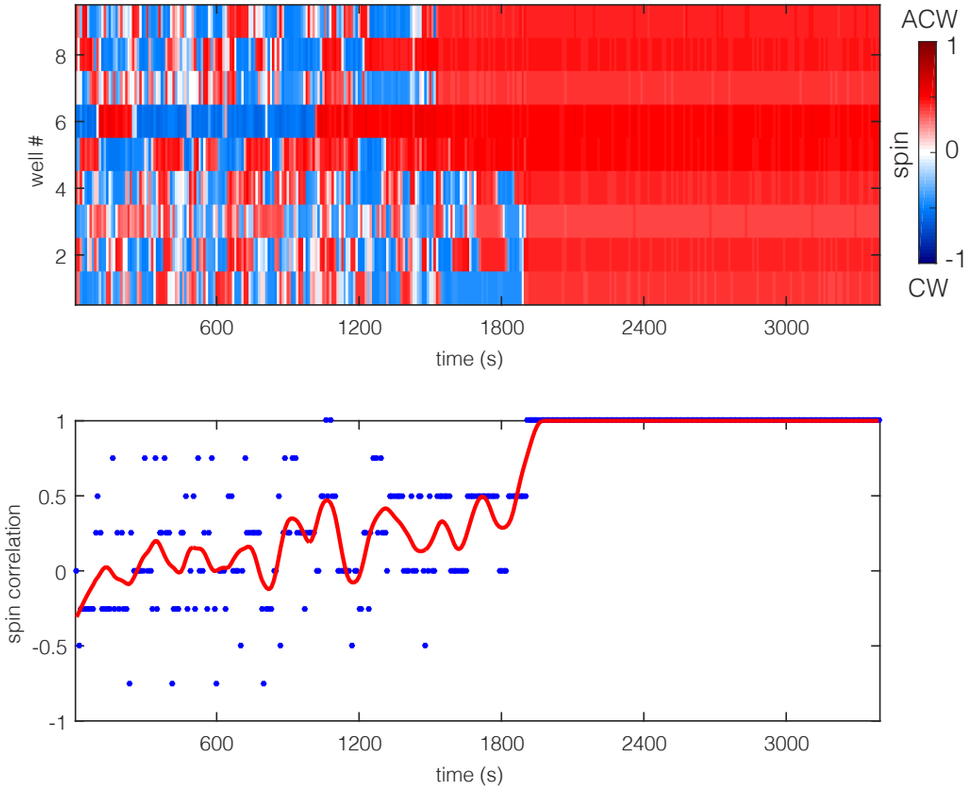

ferromagnetic

$\langle \chi \rangle > 0$

4 preferred correlated spin states

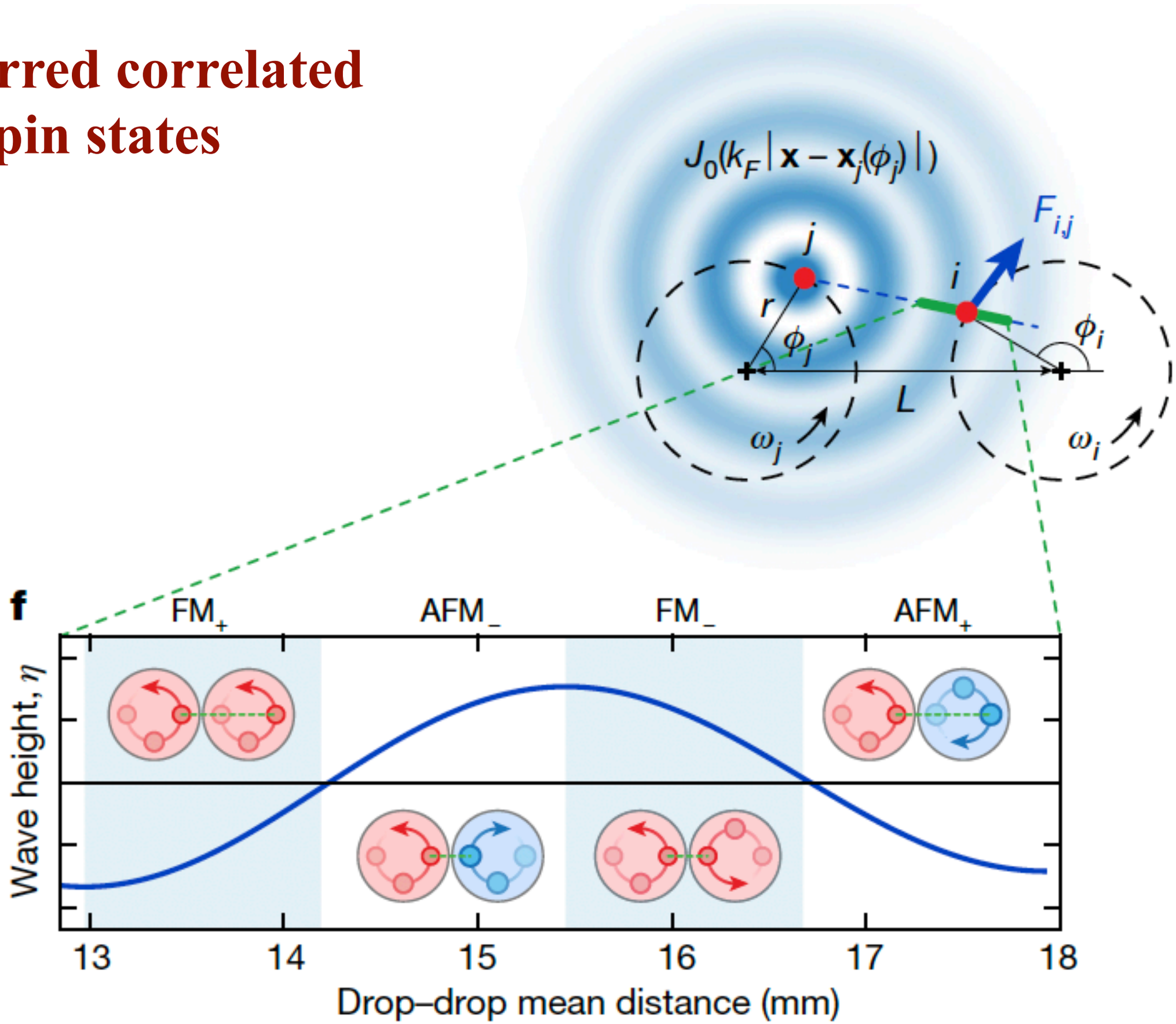

INTERACTION POTENTIAL

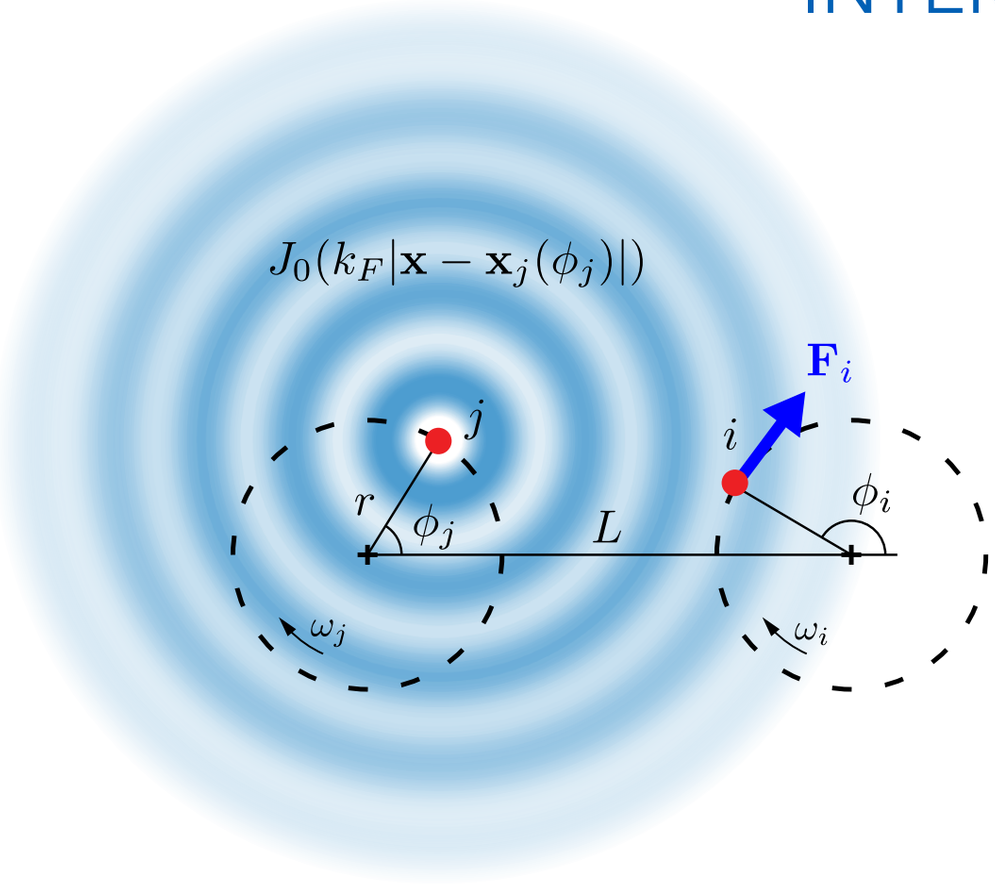

Low memory $(Me \to 0)$

$$h_j(\mathbf{x},t) = \frac{AC_f}{T_F}\int_{-\infty}^{t} J_0(k_F|\mathbf{x}-\mathbf{x}_j(s)|)e^{-\frac{(t-s)}{T_F Me}}ds$$

$$\downarrow$$

$$h_j(\mathbf{x},t) \sim J_0(k_F|\mathbf{x}-\mathbf{x}_j(\phi_j)|)$$

Circular motion

$$\mathbf{x}_j = (r\cos\phi_j, r\sin\phi_j)$$

$$\mathbf{x}_i = (L + r\cos\phi_i, r\sin\phi_i)$$

Force in direction of motion

$$F_i = -\nabla h_j(|\mathbf{x}_i(\phi_i) - \mathbf{x}_j(\phi_j)|)\cdot(-\sin\phi_i, \cos\phi_i)$$

Expand for $r \ll L$

$$F_i = A(\cos\phi_i - \cos\phi_j)\sin\phi_i - B(\sin\phi_i - \sin\phi_j)\cos\phi_i + \ldots$$

$$-\frac{\partial U}{\partial \phi_i}$$

$$U(\phi_i,\phi_j) = \alpha|\cos\phi_i - \cos\phi_j|^2 + \beta|\sin\phi_i - \sin\phi_j|^2$$

MODELING

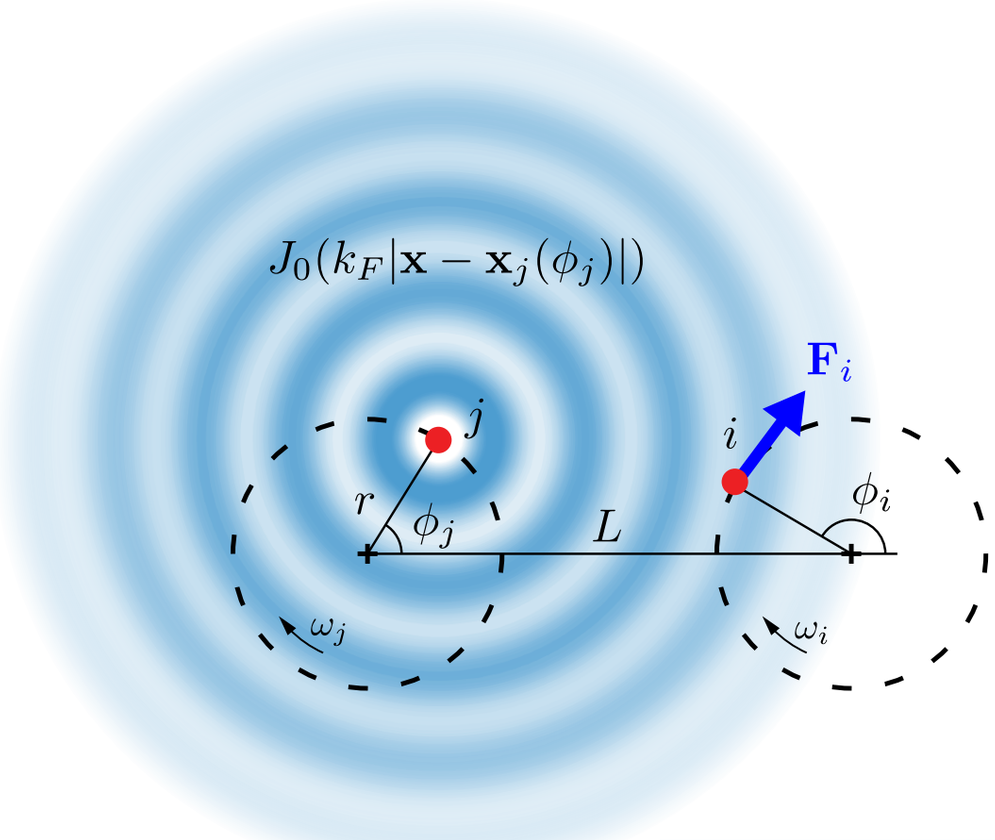

Kuramoto-like ODE model

$$\dot{\phi}_i = \omega_i$$

$$\dot{\omega}_i = \frac{1}{\tau}\left[1 - \frac{\omega_i^2}{\omega_0^2}\right]\omega_i - \sum_j \frac{\partial U}{\partial \phi_i}(\phi_i, \phi_j)$$

Preferred angular velocity

Interaction potential
(nearest neighbors)

$$U(\phi_i, \phi_j) = \alpha|\cos\phi_i - \cos\phi_j|^2 + \beta|\sin\phi_i - \sin\phi_j|^2$$

Antiferromagnetic	**Favors**	**Ferromagnetic**	**Favors**
$\alpha > 0$	Same relative x	$\alpha < 0$	Opposite relative x
$\beta < 0$	Opposite relative y	$\beta < 0$	Opposite relative y

Phase Sync

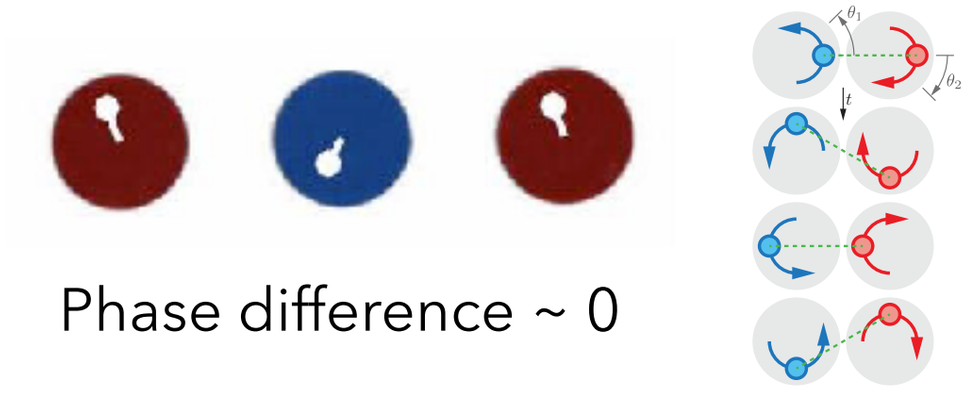

Phase difference ~ 0

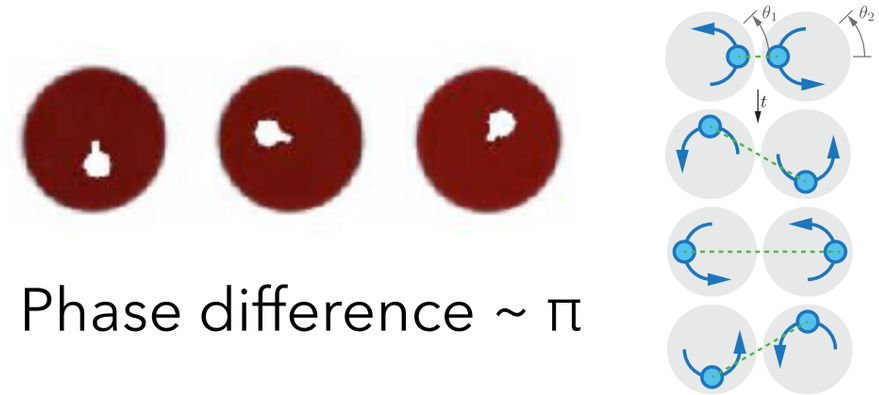

Phase difference ~ π

MECHANISM

Antiferromagnetic

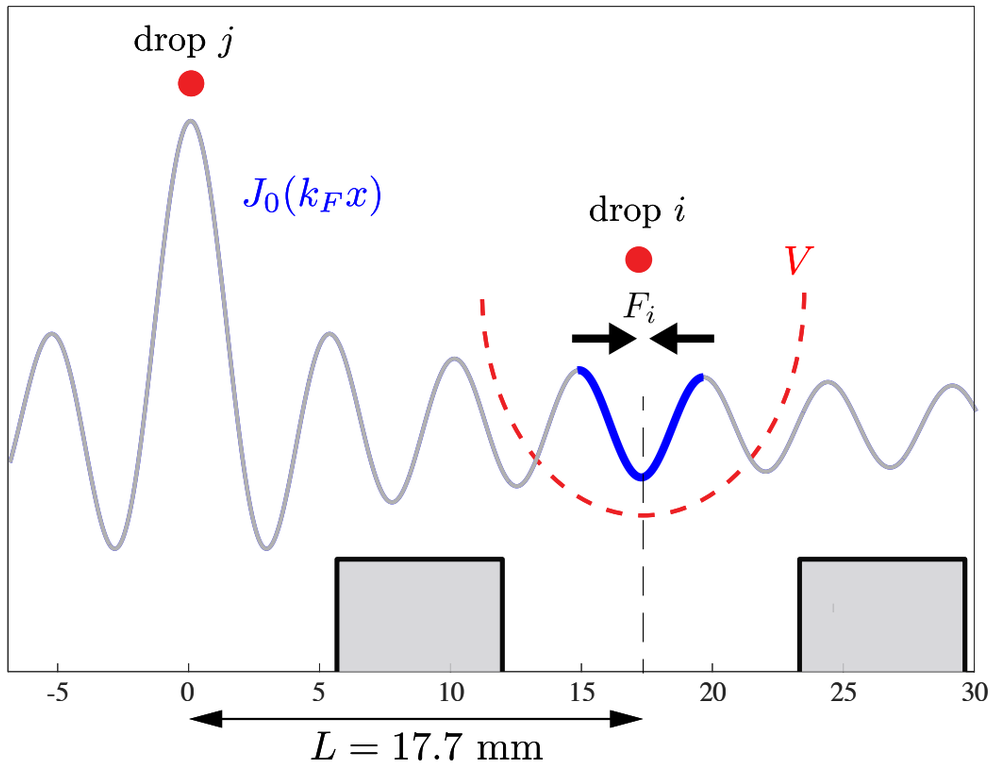

Same relative X

Ferromagnetic

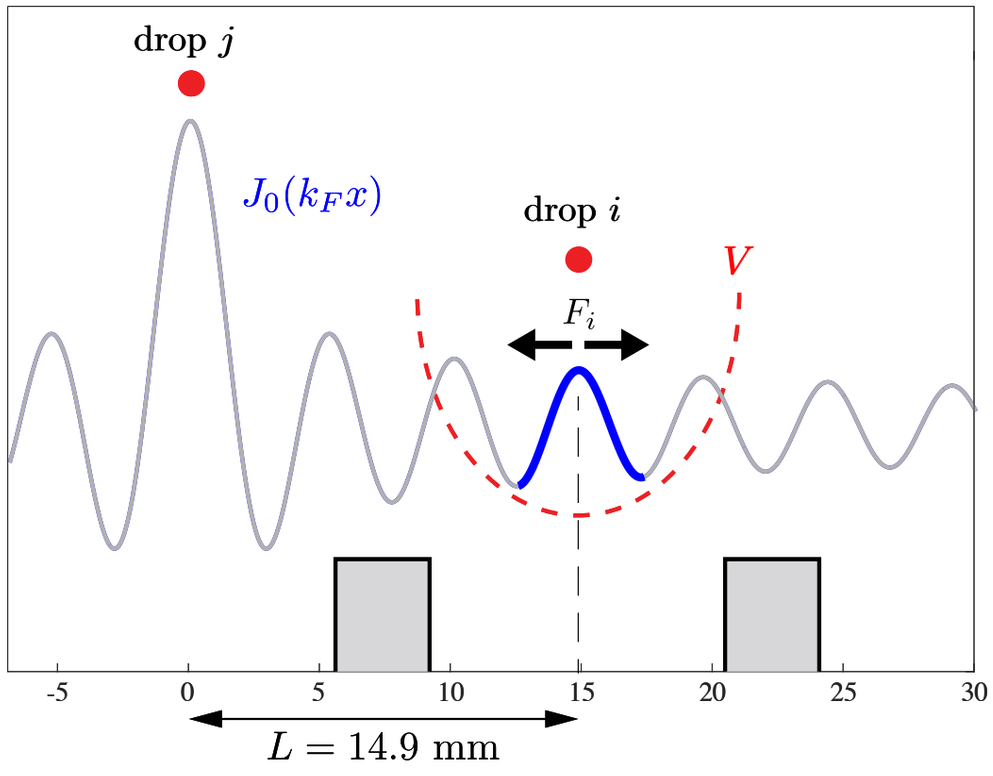

Opposite relative X

EXTERNAL FIELD

Transition to ferromagnetic order?

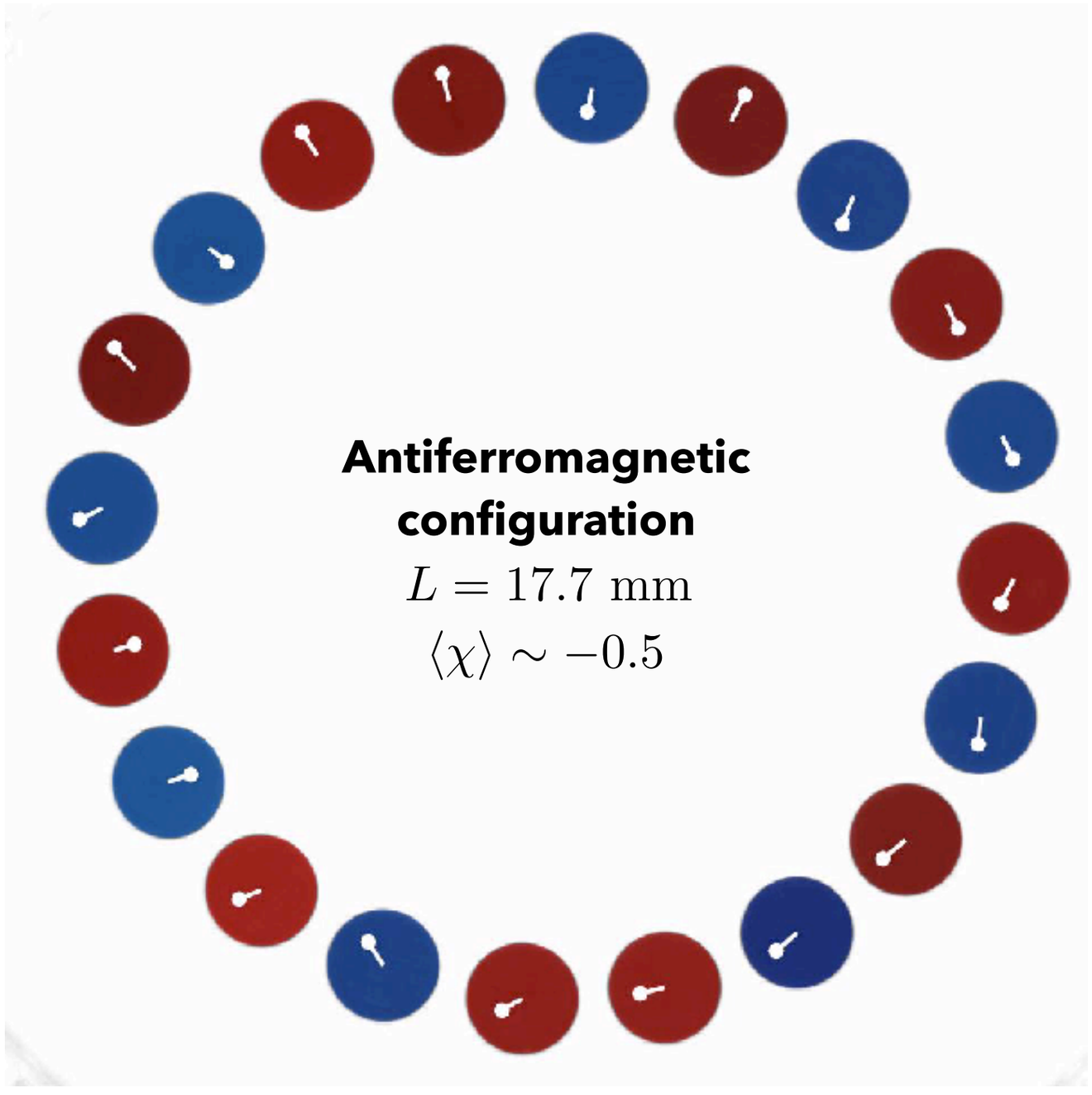

Antiferromagnetic configuration

$L = 17.7$ mm

$\langle \chi \rangle \sim -0.5$

External Field

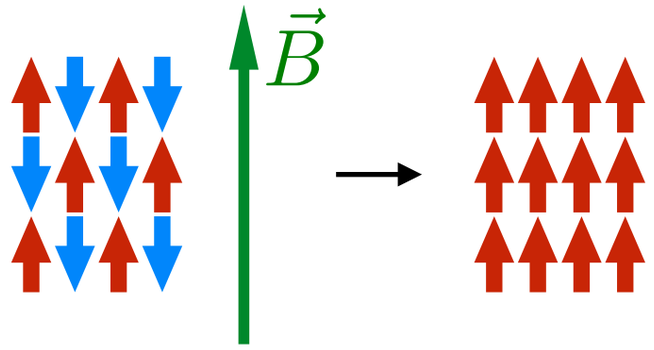

Lorentz force

on moving charge in magnetic field

$$\mathbf{F}_q = q\mathbf{v} \times \mathbf{B}$$

↕

Coriolis force

on moving mass in rotating frame

$$\mathbf{F}_C = 2m\mathbf{v} \times \mathbf{\Omega}$$

CORIOLIS FORCE AS CONTROL PARAMETER

BATH ROTATION

NO ROTATION	ANTI-CLOCKWISE	CLOCKWISE

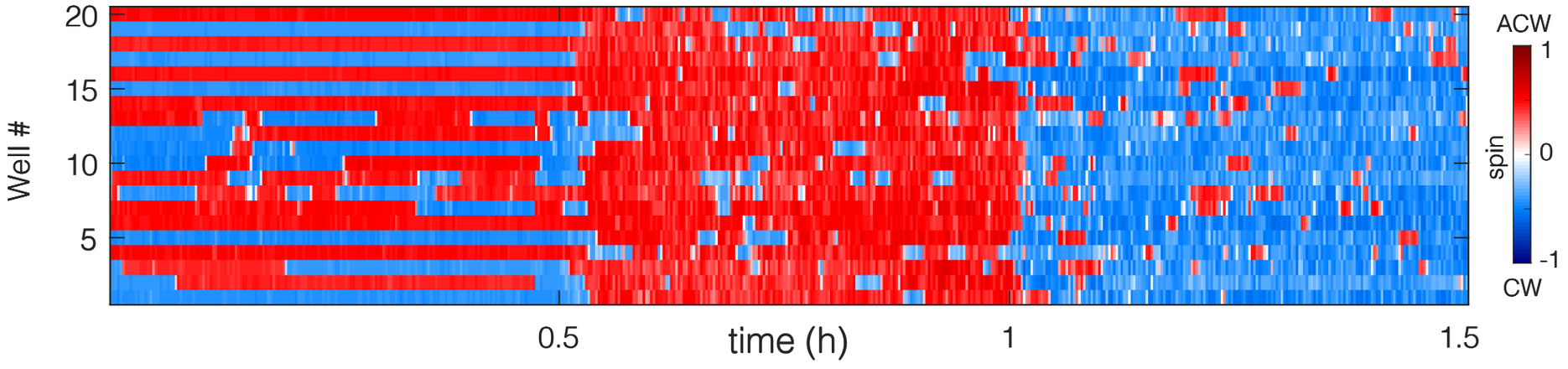

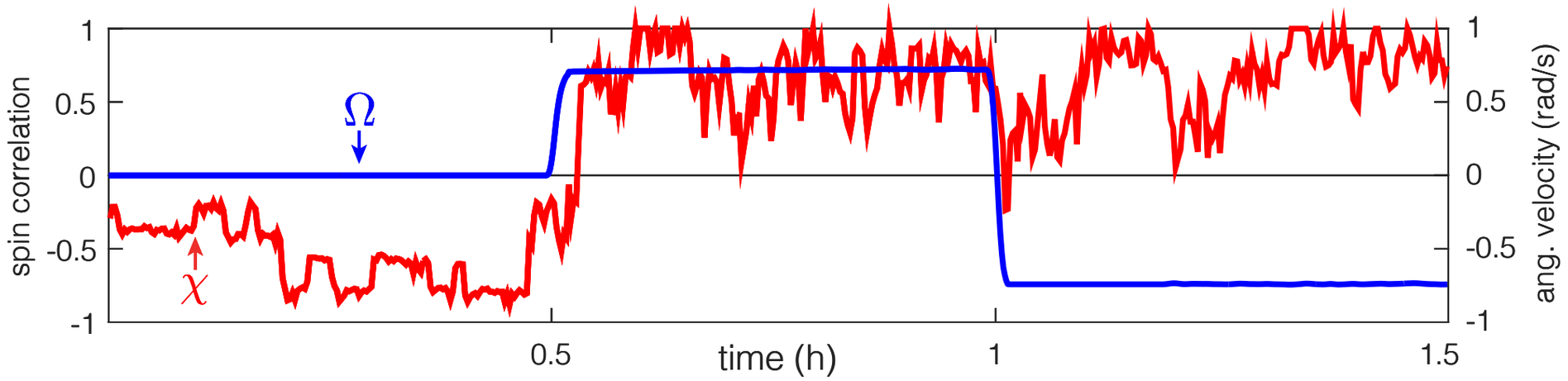

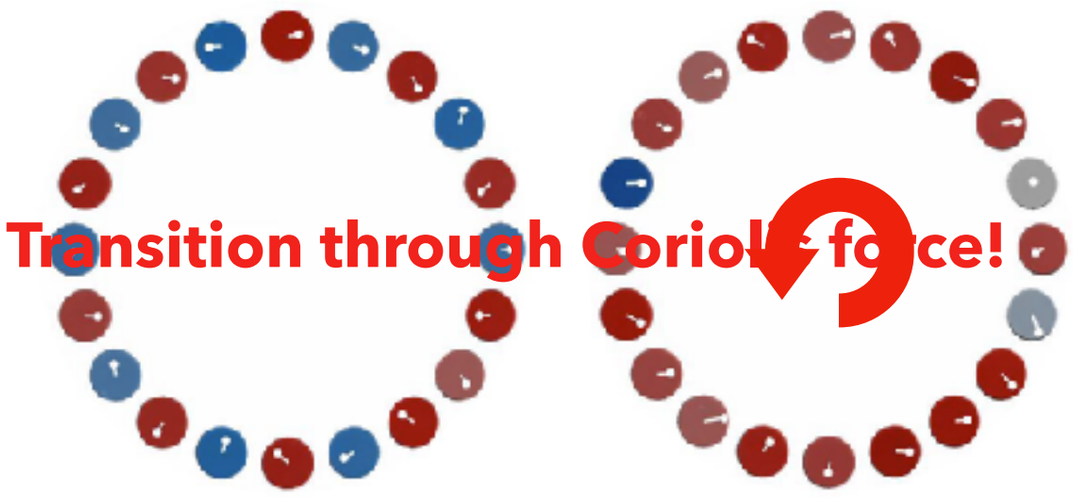

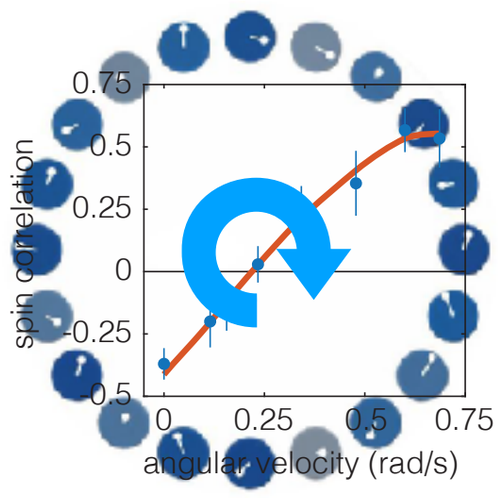

$$L = 13.2\ \mathrm{mm} \qquad \gamma/\gamma_F = 0.86$$

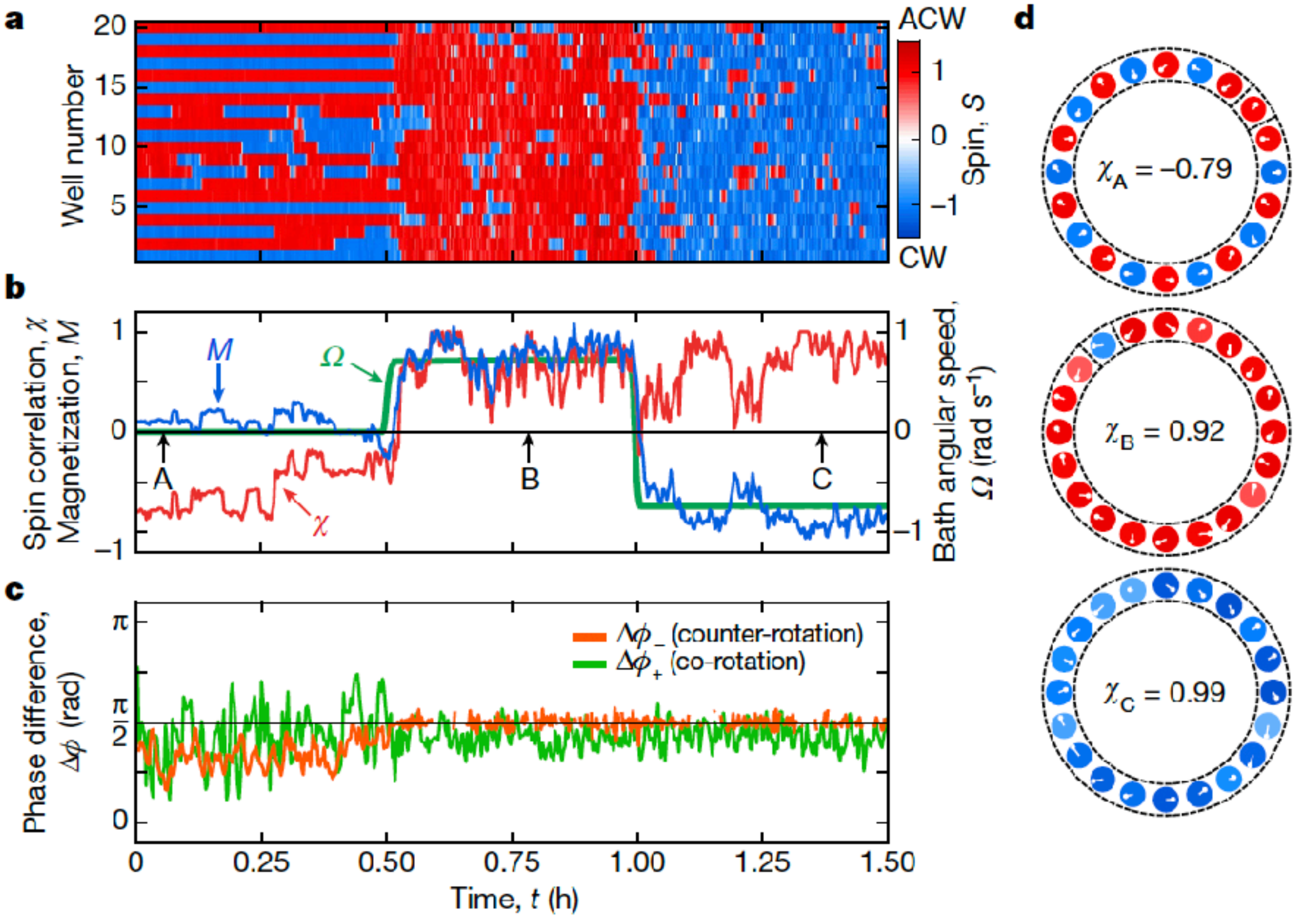

$L = 17.7$ mm $\qquad\qquad$ $\gamma/\gamma_F = 0.82$

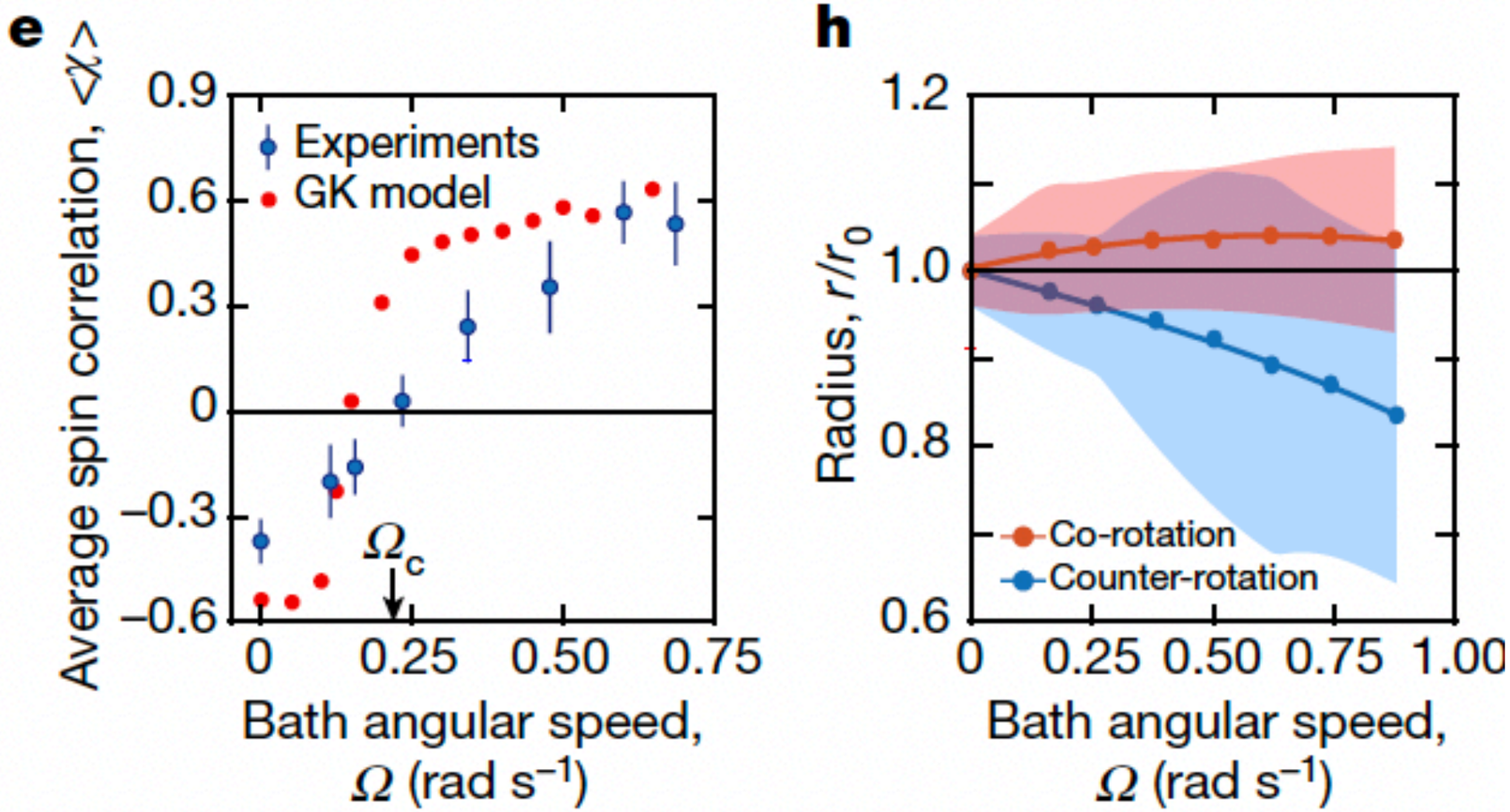

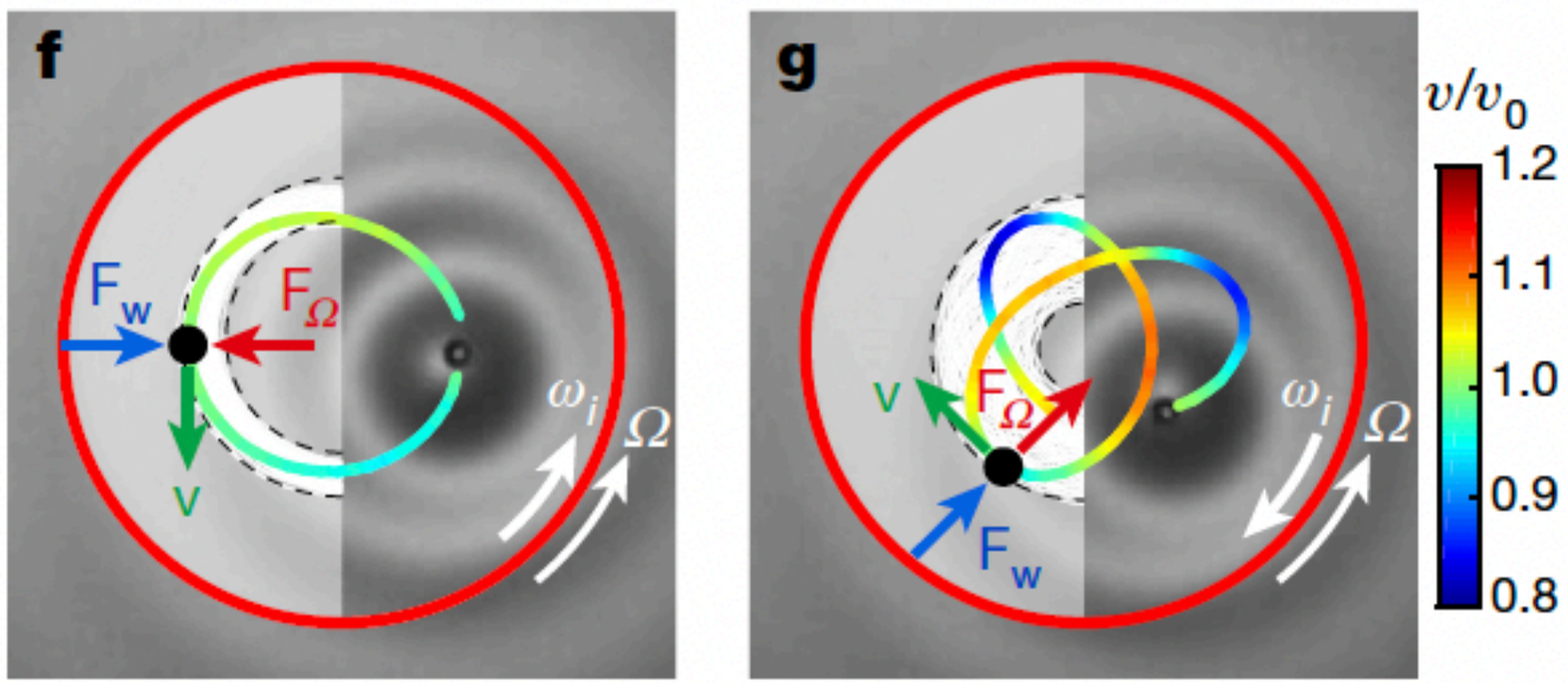

COLLECTIVE DYNAMICS IN 2D LATTICES?

$$D = 13 \text{ mm} \mid L = 17.7 \text{ mm}$$

$\Omega = 0$

$\chi \sim -0.7$

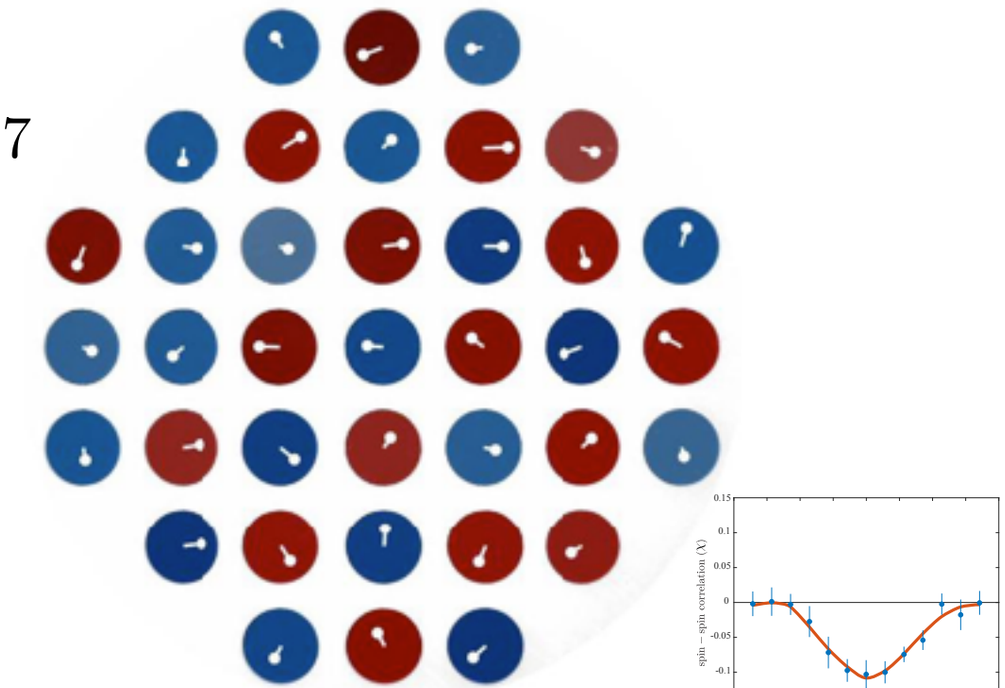

$\Omega = -0.75\,\text{rad/s}$

$\chi \sim 0.9$

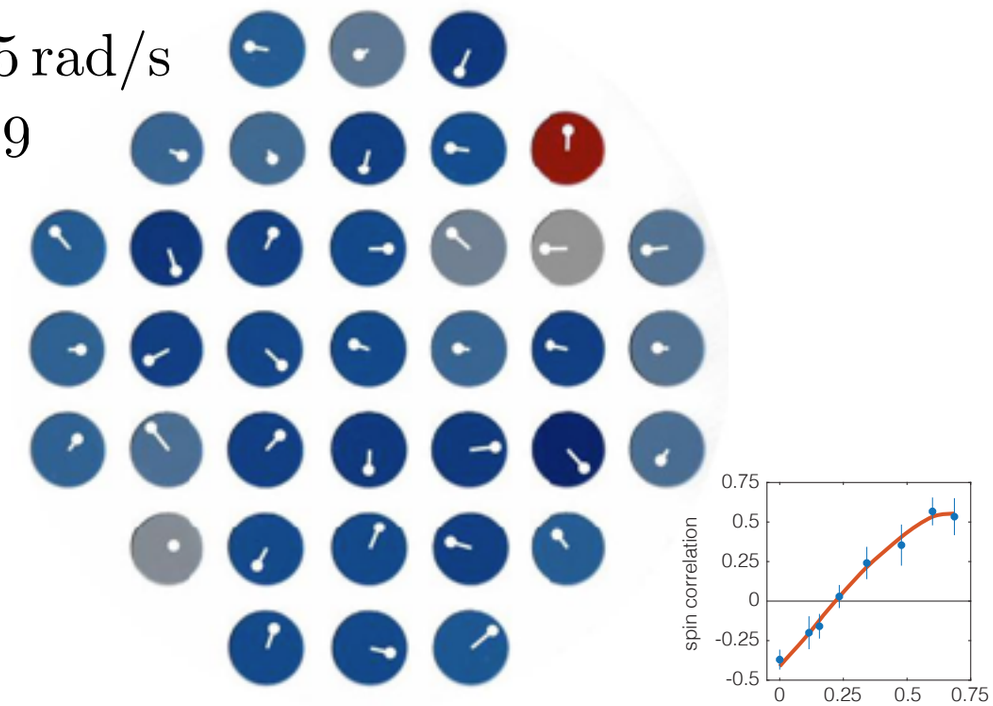

Collective dynamics are robust in 2D!

Effect of lattice geometry?

Hexagonal Lattice

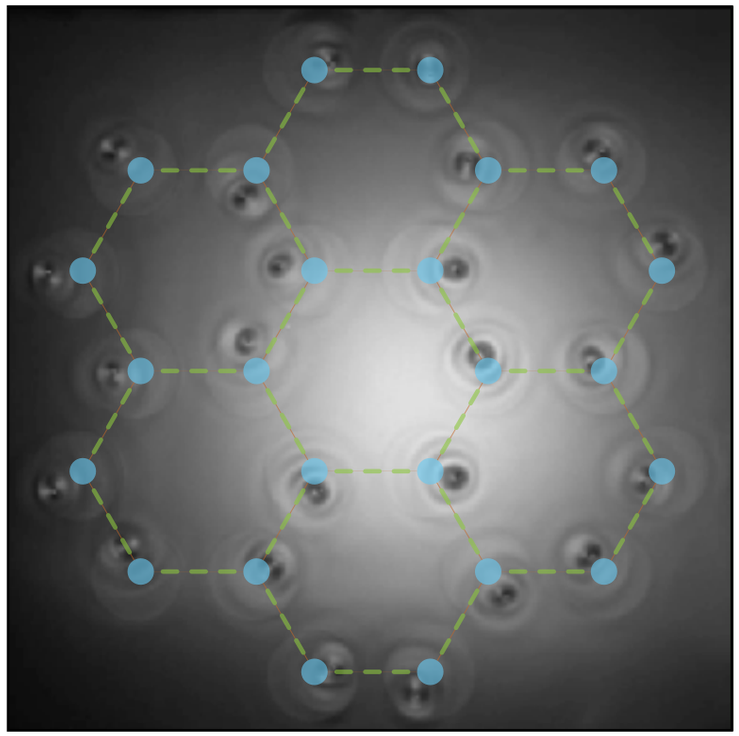

Triangular Lattice

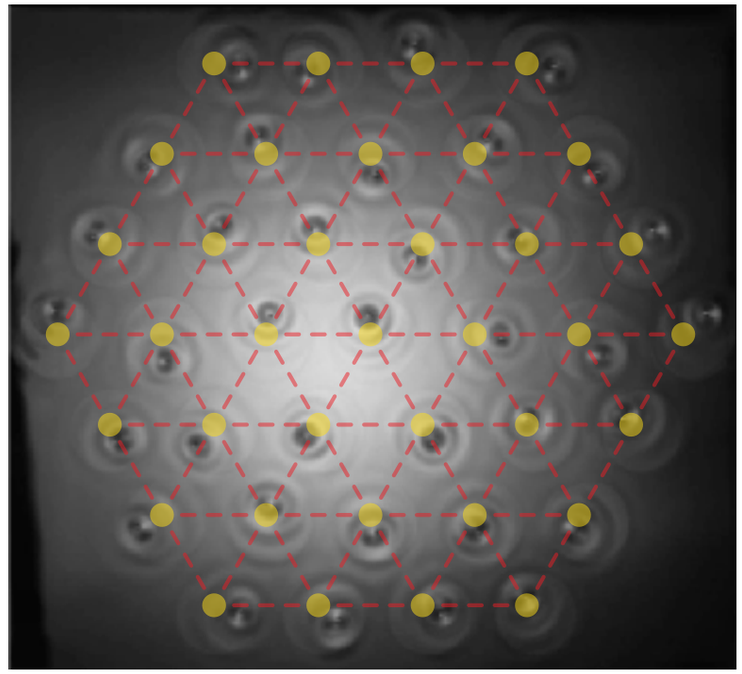

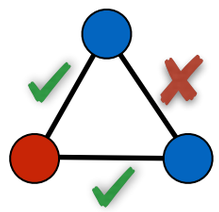

Antiferromagnetic order geometrically frustrated

Summary

- well topography may stabilize hydrodynamic spin states
- wave-mediated interactions may lead to long-range spin-spin correlations
- analog ferromagnetic and antiferromagnetic states
- correlations may be altered, reversed using system geometry and memory
- memory plays a role analogous to temperature in altering emergent states
- rotation may also prompt transitions between anti- and ferromagnetic states
- qualitative behavior captured by reduced theoretical model

Future directions

- theoretical characterization of spin waves sweeping through the lattice
- provides a possible platform for Bell tests
- current theoretical models used to justify emergent behavior are nonlocal

Walkers on shallow slopes

- droplets feel lower boundary for sufficiently shallow layers, $h < 0.6$cm

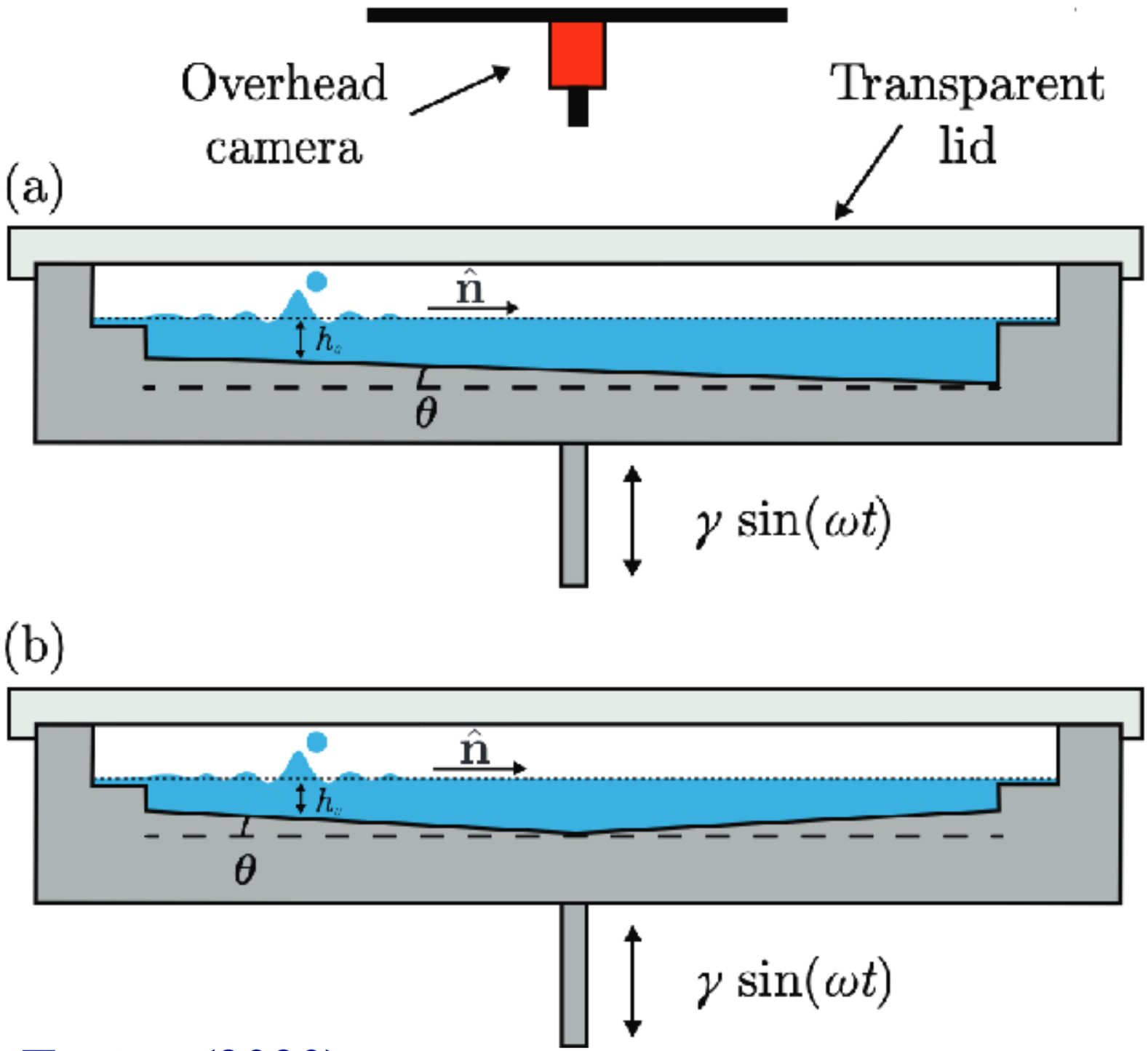

PhD of Sam Turton (2020)

Bouncer on a slope

- drift slowly into deep region, presumably to minimize dissipation

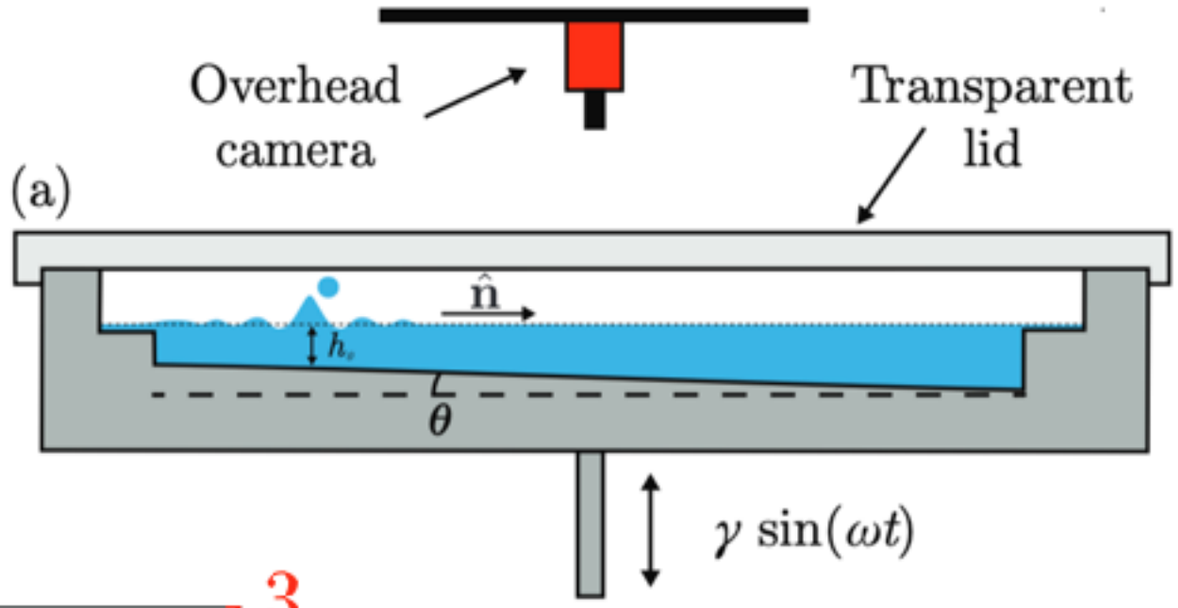

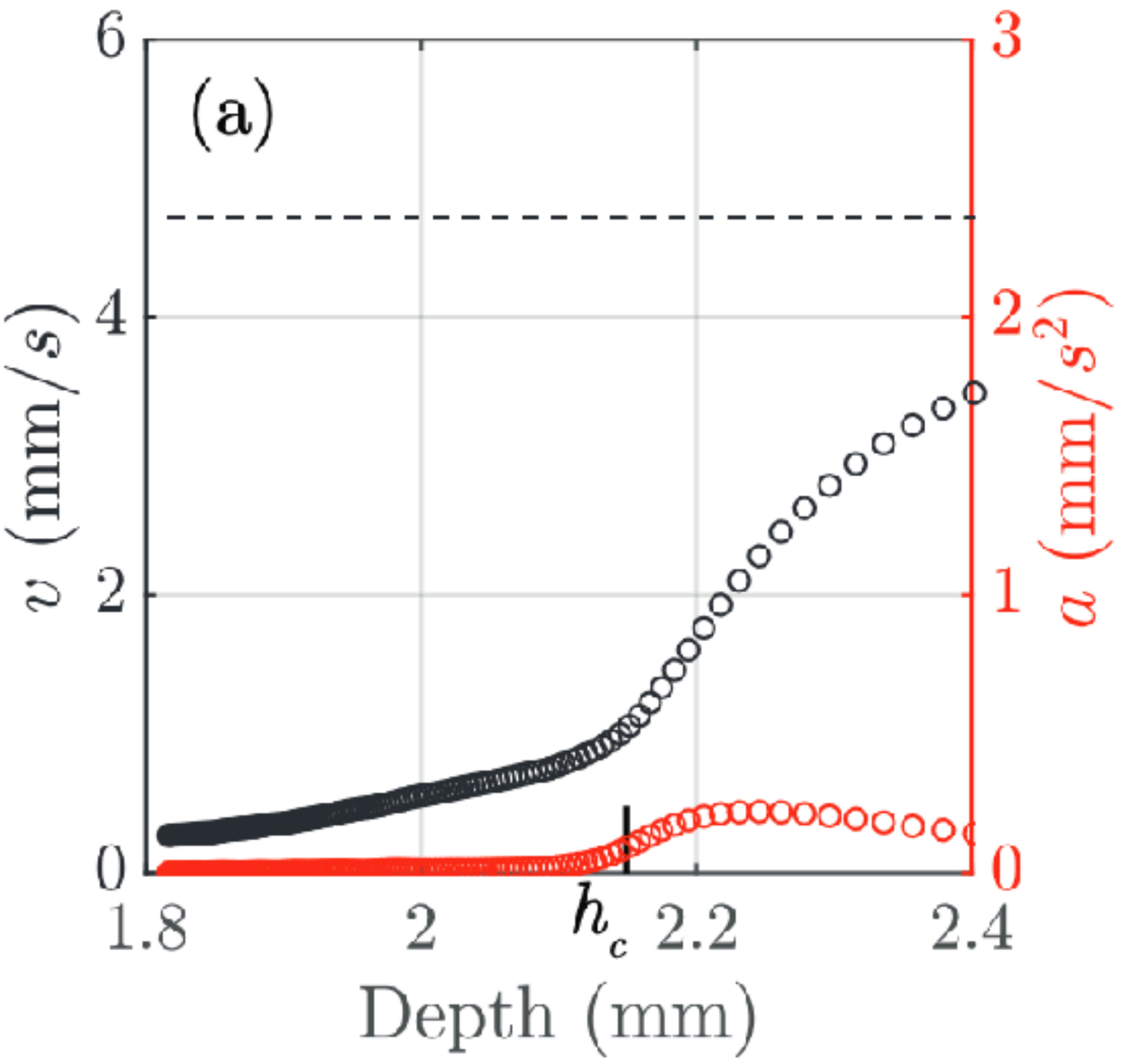

Walkers on a cone

- execute circular orbits or more complex periodic or quasiperiodic orbits

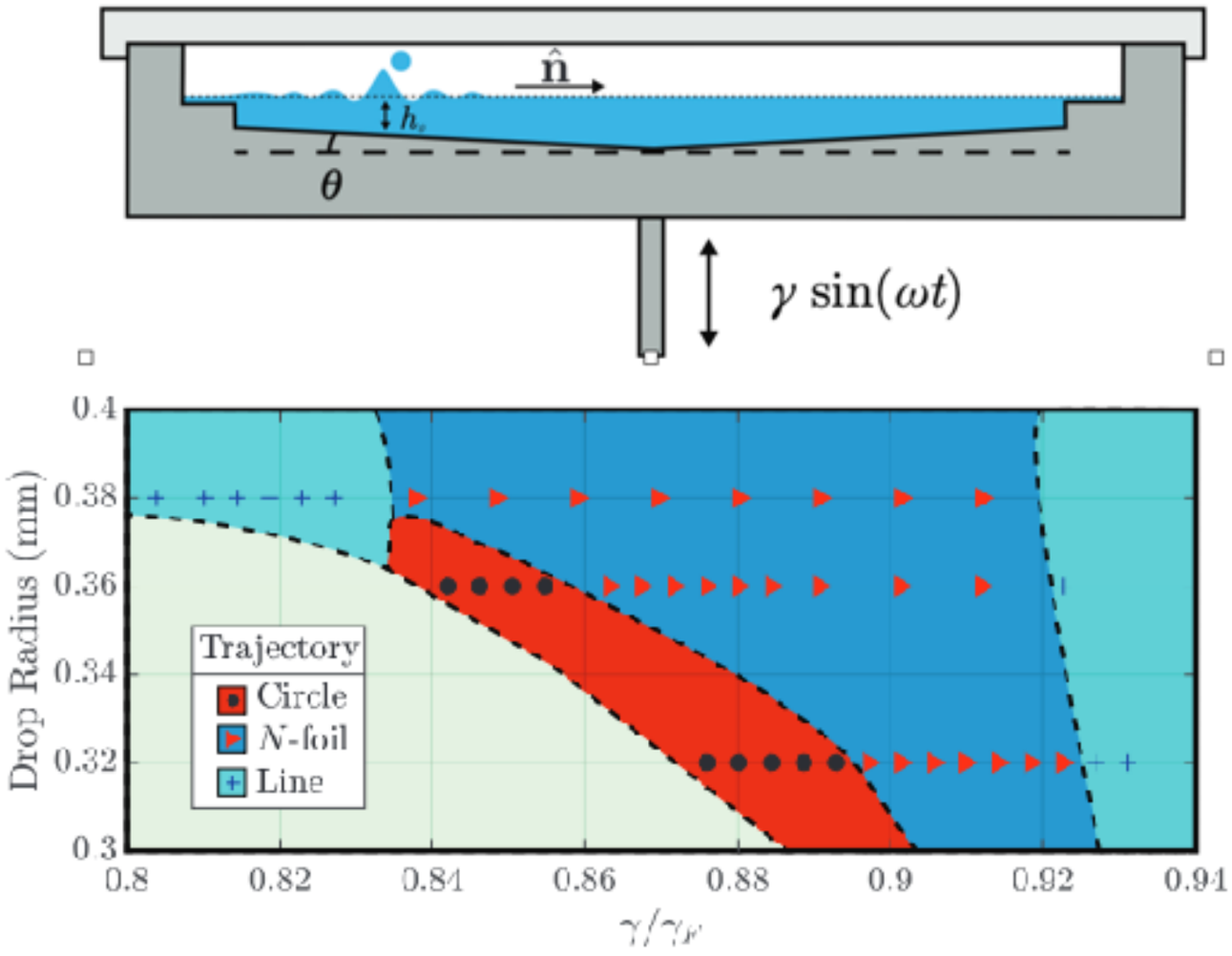

FIG. 4. A regime diagram indicating the different motions observed for droplets above conical bottom topography. Dashed lines indicate approximate transitions between different types of motion. Representative trajectories are shown in figure 5. No motion was observed in the pale green region in the lower left.

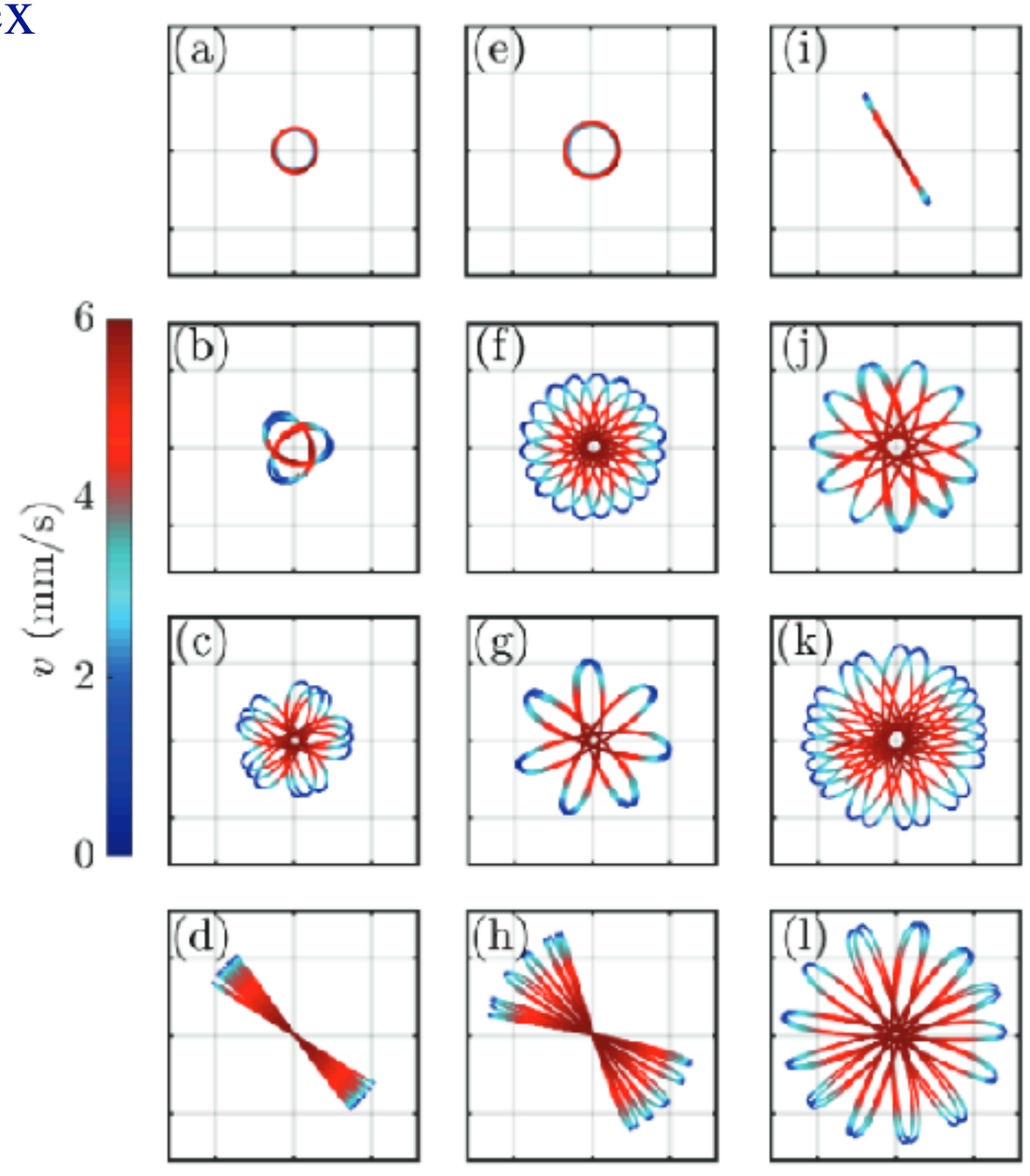

FIG. 5. Orbits arising for various drop sizes and vibrational accelerations. First column: droplets with radius $R = 0.32$ mm, with $\gamma/\gamma_F =$ a) 0.89, b) 0.9, c) 0.91 and d) 0.93. Middle column: $R = 0.36$ mm, with $\gamma/\gamma_F =$ e) 0.85, f) 0.88, g) 0.89, and h) 0.92. Third column: $R = 0.38$ mm, with $\gamma/\gamma_F =$ i) 0.83, j) 0.86, k) 0.87 and l) 0.9. The color bar at the left defines the droplet speeds. A 5 mm grid is presented for scale.

Theoretical modeling

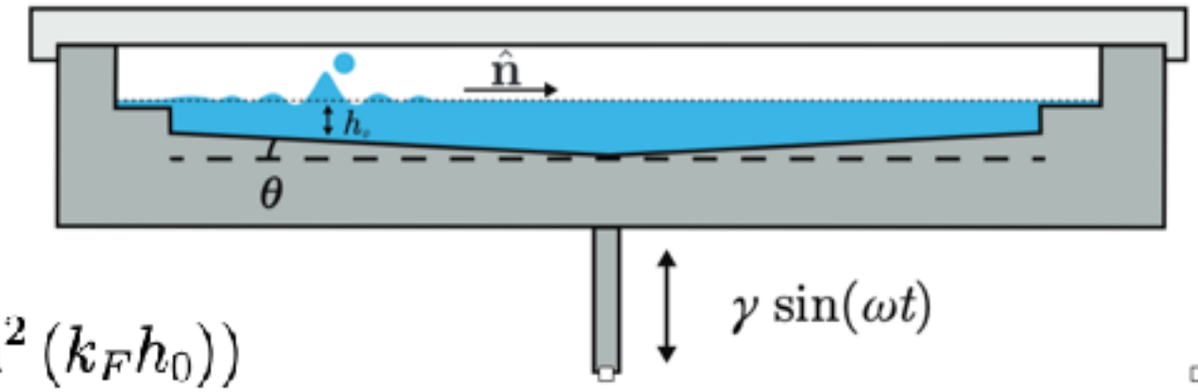

Topography: $h(\epsilon \mathbf{x}) = h_0 + \epsilon\, \mathbf{x} \cdot \hat{\mathbf{n}},$

where $\epsilon = \tan\theta \ll 1$, $\alpha = \tan\theta \dfrac{(1 - \tanh^2(k_F h_0))}{\tanh(k_F h_0)}.$

Wave form: $\eta(\mathbf{x}, t) = \dfrac{A}{T_F} \displaystyle\int_{-\infty}^{t} [1 - k_F \alpha \hat{\mathbf{n}} \cdot (\mathbf{x} - \mathbf{x}_p(s))]\, J_0(k_F |\mathbf{x} - \mathbf{x}_p(s)|) e^{-\frac{t-s}{T_M}}\, ds.$

Trajectory equation in the weak acceleration limit:

$$\frac{d}{dt}(\kappa \gamma_B \mathbf{v}) + \mathbf{v}\left[1 - \frac{\beta}{v^2}\left(1 - \frac{1}{\sqrt{1+v^2}}\right) - \frac{\alpha\beta(\mathbf{v}\cdot\hat{\mathbf{n}})}{(1+v^2)^{3/2}}\right] = \frac{\alpha\beta}{\sqrt{1+v^2}}\hat{\mathbf{n}}.$$

where $\gamma_B(\mathbf{v}) = 1 + \dfrac{\beta}{2\kappa(1+|\mathbf{v}|^2)^{3/2}}$, $\beta = \dfrac{mgAk_F^2 T_F M_e^2}{D}$

Downslope force: $\mathbf{F}_D = \dfrac{\alpha\beta}{\sqrt{1+|\dot{\mathbf{x}}|^2}}\hat{\mathbf{n}}$ drives drop into deeper fluid

Anisotropic drag: $\mathbf{D}_W = -\dfrac{\alpha\beta(\dot{\mathbf{x}}\cdot\hat{\mathbf{n}})\dot{\mathbf{x}}}{(1+|\dot{\mathbf{x}}|^2)^{3/2}}$ favors motion into deeper fluid, vanishes for azimuthal motion

Bouncer on a slope

$$\frac{d}{dt}\left(\kappa\gamma_B\mathbf{v}\right)+\mathbf{v}\left[1-\frac{\beta}{v^2}\left(1-\frac{1}{\sqrt{1+v^2}}\right)-\frac{\alpha\beta(\mathbf{v}\cdot\hat{\mathbf{n}})}{(1+v^2)^{3/2}}\right]=\frac{\alpha\beta}{\sqrt{1+v^2}}\hat{\mathbf{n}}.$$

where $\gamma_B(\mathbf{v})=1+\dfrac{\beta}{2\kappa(1+|\mathbf{v}|^2)^{3/2}}$, $\beta=\dfrac{mgAk_F^2T_FM_e^2}{D}$ $\alpha=\tan\theta\dfrac{(1-\tanh^2(k_Fh_0))}{\tanh(k_Fh_0)}$.

Seek drifting solution: $\mathbf{x}_p(t)=u_Dt\hat{\mathbf{n}}$

$$u_D\left[1-\frac{\beta}{u_D^2}\left(1-\frac{1}{\sqrt{1+u_D^2}}\right)-\frac{\alpha\beta u_D}{(1+u_D^2)^{3/2}}\right]=\frac{\alpha\beta}{\sqrt{1+u_D^2}} \quad \longrightarrow \quad u_D=\alpha\beta$$

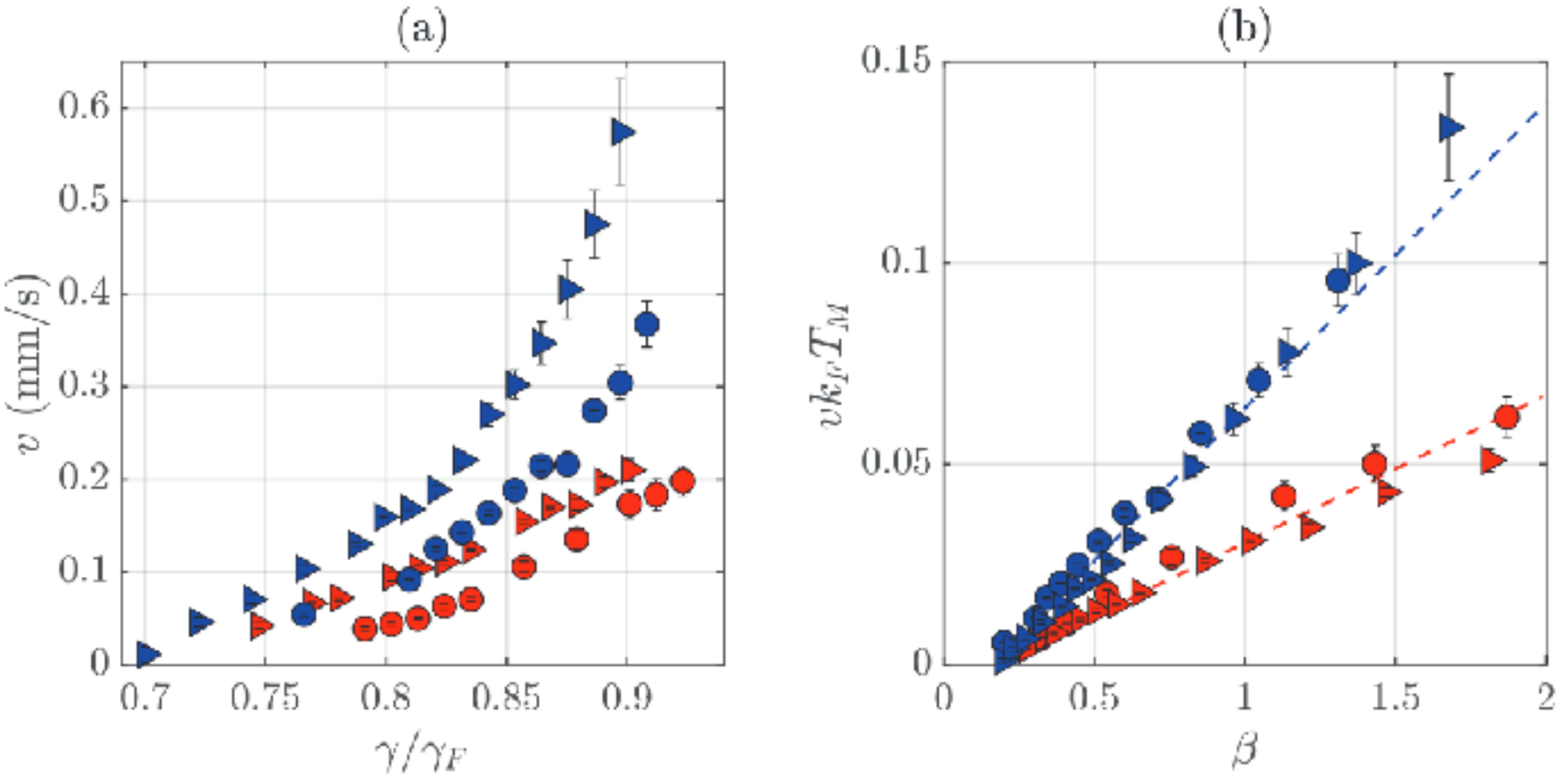

Bouncer on a cone

$$\frac{d}{dt}\left(\kappa\gamma_B\mathbf{v}\right)+\mathbf{v}\left[1-\frac{\beta}{v^2}\left(1-\frac{1}{\sqrt{1+v^2}}\right)-\frac{\alpha\beta(\mathbf{v}\cdot\hat{\mathbf{n}})}{(1+v^2)^{3/2}}\right]=\frac{\alpha\beta}{\sqrt{1+v^2}}\hat{\mathbf{n}}.$$

where $\gamma_B(\mathbf{v})=1+\dfrac{\beta}{2\kappa(1+|\mathbf{v}|^2)^{3/2}}, \qquad \alpha=\tan\theta\dfrac{(1-\tanh^2(k_Fh_0))}{\tanh(k_Fh_0)}.$

Seek orbital solutions: $\mathbf{x}_p(t)=r_0\left(\cos\omega t,\sin\omega t\right)$

$$\kappa\gamma_B r_0\omega^2=\frac{\alpha\beta}{(1+(r_0\omega)^2)^{1/2}},$$

$$r_0\omega=\frac{\beta}{r_0\omega}\left(1-\frac{1}{\sqrt{1+(r_0\omega)^2}}\right)$$

To find: $u_0\equiv|r_0\omega|=\dfrac{1}{\sqrt{2}}\left(-1+2\beta-\sqrt{1+4\beta}\right)^{1/2}$ free walking speed

Orbital frequency $\omega=\dfrac{\pm\alpha\beta}{\kappa\gamma_B u_0\sqrt{1+u_0^2}}$ and radius $r_0=\dfrac{\kappa\gamma_B u_0^2\sqrt{1+u_0^2}}{\alpha\beta}$

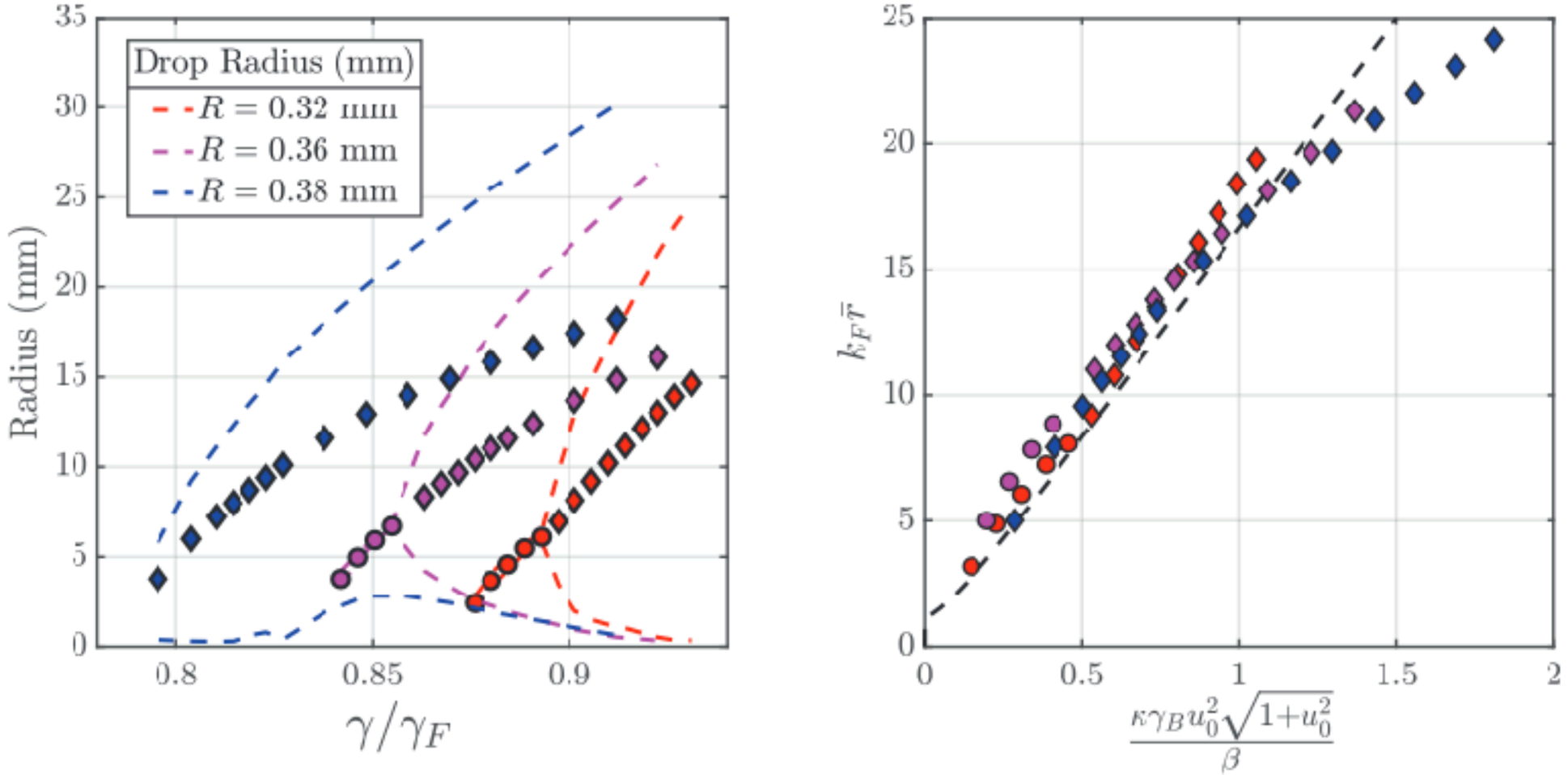

FIG. 6. (a) Dependence of the time-averaged mean radius on the normalized vibrational acceleration γ/γ_F, for each of the three drop sizes. Dashed lines indicate the minimum and maximum distance from the origin attained on these trajectories. (b) Dependence of the non-dimensional observed mean radius, $k_F\bar{r}$, on the dimensionless group $\frac{\kappa\gamma_B u_0^2\sqrt{1+u_0^2}}{\beta}$. Phase parameters of $\sin\Phi = 0.25, 0.3$ and 0.45 were used for droplets with radius $R = 0.32, 0.36$ and 0.38 mm respectively, in order to match the onset of motion with the walking threshold γ_W. These are in line with values used in previous studies [43, 47]. The dashed curve indicates a line of best-fit, with slope 0.06. Circles denote circular trajectories; diamonds denote all others.

Summary

- slowly-varying topography difficult to model: spatially dependent memory
- topography induces down-slope force and anisotropic drag
- conical bottom topography supports orbital motion

Interesting question

To what extent can we think of topographic anomalies as the generators of forces?

- only in a limited number of special cases

  E.g.1 Walkers interacting with pillars, wells

  E.g.2 Walkers orbiting above a conical substrate

- force generally depends on history, manner of approach